ABSTRACT

AM/FM DIGITAL AUDIO BROADCASTING
In-Band On-Channel
Transmission

by
Michael Meyer

This thesis examines the in-band on-channel transmission of digital audio data for application in Digital Audio Broadcasting (DAB). The premise is to use the existing FM channels for transmission of DAB. For the FM channel used for analog audio transmission, two different scenarios are suggested and investigated.

In the first scenario, to enable overlay of the new DAB and current FM transmissions, the digital data is modulated by a direct sequence spread spectrum signal to bring the average transmitted power below that of the FM signal using the same channel. The FM signal interferes with the digital transmission and it needs to be excised before the digital signal can be decoded. Different excision techniques, such as a fixed subband-based exciser, an adaptive subband-based exciser, and a Binomial-Gaussian window-based exciser, are suggested and their performances evaluated.

The second FM scenario involves transmitting the digital audio data as an AM modulation on the FM signal. Since the FM receiver evaluates the phase information only, the additional envelope modulation does not interfere with the analog FM service.

In addition to the FM channel investigation, a preliminary analysis of the use of the AM channel for digital overlay transmission is presented.

AM/FM DIGITAL AUDIO BROADCASTING IN-BAND ON-CHANNEL TRANSMISSION

by
Michael Meyer

A Thesis
Submitted to the Faculty of
New Jersey Institute of Technology
in Partial Fulfillment of the Requirements for the Degree of
Master of Science in Electrical Engineering

Department of Electrical and Computer Engineering

January 1995

APPROVAL PAGE

AM/FM DIGITAL AUDIO BROADCASTING IN-BAND ON-CHANNEL TRANSMISSION

Michael Meyer

Dr. Ali N. Akansu, Thesis Advisor — Date
Associate Professor of Electrical
and Computer Engineering, NJIT

Dr. Alexander Haimovich, Committee Member — Date
Associate Professor of Electrical
and Computer Engineering, NJIT

Dr. Zoran Siveski, Committee Member — Date
Assistant Professor of Electrical
and Computer Engineering, NJIT

BIOGRAPHICAL SKETCH

Author: Michael Meyer

Degree: Master of Science in Electrical Engineering

Date: January 1995

Undergraduate and Graduate Education:

- Master of Science in Electrical Engineering,
  New Jersey Institute of Technology, Newark, New Jersey, 1995

- Diplom Ingenieur Nachrichtentechnik (FH),
  Fachhochschule der Deutschen Bundespost Telekom Dieburg,
  Germany, 1993

Major: Electrical Engineering

Presentations and Publications:

Michael Meyer, Mehmet V. Tazebay, and Ali N. Akansu, "A Sliding and Variable Window-Based Multitone Excision for Digital Audio Broadcasting," submitted to *IEEE International Symposium on Circuits and Systems*, April 26 to May 8, 1995, Seattle, Washington.

I would like to dedicate this thesis to my family,
for the endless support they gave me
during my time at NJIT.

ACKNOWLEDGMENT

I would like to express my gratitude toward my advisor Dr. Ali N. Akansu for his support and guidance throughout the research period. Special thanks to Dr. Alexander Haimovich and Dr. Zoran Siveski for serving as committee members.

I am very grateful to Mehmet Tazebay for his time and effort he spend discussing and helping to improve this work. Thanks are also due to Dr. Abdulkadir Dinç for his valuable advice and input.

This work would not have been possible without the generous support of the Fulbright Commission, which enabled me to study in the United States, as well as gain insight into a new culture, its problems and the beauty of the country.

A special thanks to Lisa Fitton, Murat Berin and all of my friends and family for their support throughout my entire stay in the U.S.

TABLE OF CONTENTS

Chapter	Page

LIST OF TABLES

LIST OF FIGURES

Figure		Page

Figure	Page

LIST OF ABBREVIATIONS

Abbreviation	Term
AWGN	Additive White Gaussian Noise
BPSK	Binary Phase Shift Keying
CD	Compact Disc
CDMA	Code Division Multiple Access
COFDM	Coded Orthogonal Frequency Division Multiplexing
DAB	Digital Audio Broadcasting
DCT	Discrete Cosine Transform
DFT	Discrete Fourier Transform
DSSS	Direct Sequence Spread Spectrum
FCC	Federal Commission on Communication
FDMA	Frequency Division Multiple Access
FIR	Finite Impulse Response
FM	Frequency Modulation
GLT	Generalized Linear Transform
KLT	Karhunen-Loeve Transform
MUSICAM	Masking pattern Universal Subband Integrated Coding and Multiplexing
NRZ	Not Return to Zero
PLL	Phase Lock Loop
PR	Perfect Reconstruction
PSD	Power Spectral Density
QMF	Quadrature Mirror Filter
QPSK	Quadrature Phase Shift Keying
R&D	Research and Development

Abbreviation	Term
RF	Radio Frequency
SNIR	Signal to Noise and Interference Ratio
SNR	Signal to Noise Ratio
SPW	Signal Processing WorkSystem
TDMA	Time Division Multiple Access
VCO	Voltage Controlled Oscillator

CHAPTER 1

INTRODUCTION

Digital Audio Broadcasting (DAB) allows the transmission of high quality digital audio to the public. The motivation for analog radio broadcasters for this new technology lies competing with recently introduced digital equipment in home and car audio markets. Since more radio listeners switch to digital audio, even during the daily commute, the audience for the analog conventional AM and FM broadcasters is steadily declining over the last few years.

The first contribution to digital audio broadcasting development was made by a joint project among various European governments and companies. This project, which is known as EUREKA-147, started to study a DAB standard for Europe in January 1988. After testing different options, the EUREKA-147 group chose [9] MUSICAM source coding, COFDM modulation, and unequal convolutional error protection for their recommended DAB-system.

The MUSICAM algorithm is a subband coding-based data reduction technique. It is capable of compressing CD-quality audio (approximately 1,411 KBits/s) at a data rate as low as approximately 100 KBits/s. In ISO-testings, a MUSICAM algorithm proved to be subjectively indistinguishable from the original audio at a data rate of 256 KBits/s.

The digital modulation scheme chosen by EUREKA-147 was an orthogonal multi-carrier system. This decision was based on the study of characteristics of multipath reflections in VHF systems. Reflections in VHF systems commonly occur within a time delay of 10 μs. If the symbol length is long enough compared with such multipath effects, these interferences are negligible. Therefore, the symbols must have a length of $100 - 200 \mu s$. One way of achieving the required bit rate is to use

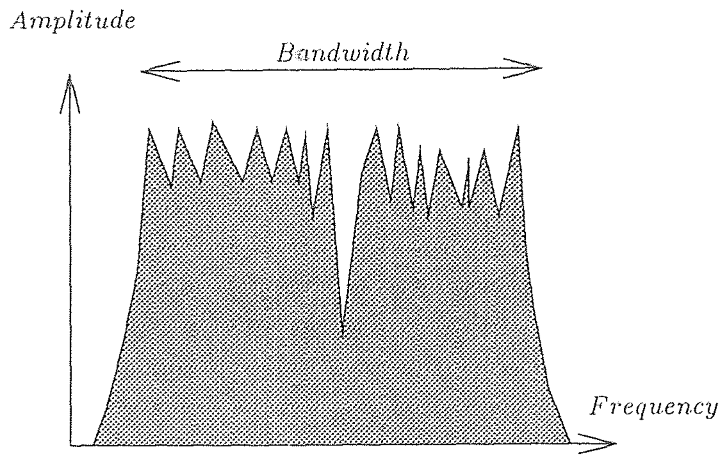

Figure 1.1 Notch caused by Multipath Interference

many orthogonal carriers in parallel to transmit the data. This technique introduces a second multipath interference protection into the system; namely, frequency diversity. The multipath reflections normally introduce a notch into the frequency spectrum, as displayed in Fig. 1.1. If more carriers are employed, the effects of this narrow-band notch are reduced.

The channel coding of the EUREKA-147 system is a convolutional code with a soft decision Viterbi decoder [9]. The coding rate varies according to the relative subjective importance of the audio frame from 1/4 to 3/8 with an effective coding rate of 1/2.

So, why not to adapt this standard in the United States?

There are some differences between the U.S. and European broadcasting systems. In Europe, most stations broadcast using public facilities. Hence the public broadcasters can reach many common listeners. In the United States, broadcasters have to compete in the advertisement market. Therefore, the number of listeners automatically determines the advertising revenues. The EUREKA-147 system puts 5-16 broadcasters into one carrier group. This mandatory grouping conflicts with the competition existing between stations in the United States. The second drawback is that the EUREKA-147 standard requires an available bandwidth of approximately 50MHz for the DAB in the United States. This bandwidth is unavailable in today's crowded frequency spectrum. The European countries solved this problem by assigning different frequencies (e.g., unused TV channels) to different countries. This causes receivers to be more complex than a simple radio receiver with a common frequency band for all countries. Therefore, the task is to establish a system that combines the transmission properties of the European system, while considering the bandwidth limitations of the United States. Currently, different R&D companies are working on this new technology. The first group of candidate systems are being presently tested by the FCC. There is still a need for new ideas to improve these systems.

This thesis examines different transmission techniques for AM and FM DAB. The transmission of digital audio data in-band on-channel can be established by using phase modulation techniques. The normal AM-receiver does not make use of the phase information. Therefore, the digital data is phase encoded and a special receiver recovers the information. Since the conventional receiver uses non coherent reception techniques, the transmission is not disturbed. The FM DAB discussed in this thesis is using either a AM-modulation on the FM signal or a direct spread spectrum signal beneath the analog FM. The AM transmission uses the amplitude for adding the digital audio information. Since the conventional FM receivers don't recover any amplitude information, they are unaffected by this technique. In case of the DSSS the disturbing effects of the analog FM signal have to be reduced. Therefore we will present some excision techniques capable of excising multiple interferences. On exciser uses the Binomial Gaussian Window filter to excise the interferences. The filter function is adapted to the special needs of the spectrum and a excision margin ensures that the excision is stopped when a optimal point is reached.

CHAPTER 2

SPREAD SPECTRUM THEORY

2.1 Spread Spectrum Systems

Spread spectrum systems were first used for military communication purposes. These communication systems must be resistant against possible unintended receivers. They should have a low probability of intercept, and high protection against distortions caused by natural and artificial sources, such as noise and jamming. All of these system requirements can be solved if the signal is represented by a noise-like wide-band signal through the channel. In this case the bandwidth of the signal is much wider than the original data spectrum. This increased bandwidth requirement is of minor concern for military applications. But it causes some problems in commercial communications systems, where the bandwidth and power are the main concerns. We will focus on a commercial application of spread spectrum techniques in this thesis.

2.1.1 The Advantages of Using Spread Spectrum Systems

The basic idea of spread spectrum systems is to extend the data bandwidth in order to gain protection against distortion or to provide multi-user access to the channel. This bandwidth extension is realized by multiplying the data bits with a spreading sequence. The spreading sequences are introduced later in this chapter. The length of such a sequence N is called the chip rate. The chip duration is $T_c = \frac{T_d}{N}$, where T_d is the data bit length.

2.1.1.1 Interference Rejection

The advantages of spreading for interference rejection is displayed in Figure 2.1. The DSSS transmitter spreads the data sequence d_l where $(d_l \in \{-1, 1\}$,

$\forall l$) and therefore its bandwidth by multiplying it with the spreading sequence $\underline{c}$ ($c_i \in \{-1, 1\}$, for $i = 1, ..N$). During transmission the channel adds noise $\underline{n}_l$ and other interferences $\underline{j}_l$. At the receiver side, the received signal $\underline{r}_l$ is expressed as

$$\underline{r}_l = d_l \underline{c} + \underline{j}_l + \underline{n}_l. \tag{2.1}$$

The receiver multiplies the received signal with a properly synchronized version of the spreading sequence $\underline{c}$. The length-N pseudonoise (PN) spreading code has the energy, $\underline{c}\,\underline{c}' = \sum_{i=1}^{N} c^2(i) = N$. The decision variable is given by,

$$\begin{aligned} U_l &= \underline{r}_l\,\underline{c}' = d_l \underline{c}\,\underline{c}' + \underline{j}_l\,\underline{c}' + \underline{n}_l\,\underline{c}' \qquad (2.2) \\ &= N d_l + \underline{j}_l\,\underline{c}' + \underline{n}_l\,\underline{c}'. \end{aligned}$$

This shows that the despreading operation spreads the interfering signals while recovering the data. This spread of the interferences causes a significant loss of interfering power at the demodulator. Therefore, the data recovery is much less likely to produce errors than without spreading. This reduction of interferences is expressed in the process gain of a spread spectrum system. If the data d_l has significant power within $W_d = \frac{1}{T_d}$, and we are chipping it with a sequence of length $N = \frac{T_d}{T_c}$, where T_c is the bit duration of the spread signal, then the despreading operation causes an interference of bandwidth W_I to be spread over NW_I. This means that the ratio of the original interference power to the interference power after despreading within the data bandwidth is given as

$$G = 10 \log \frac{P_I}{\frac{P_I}{N}} = 10 \log \frac{T_d}{T_c} = 10 \log N, \tag{2.3}$$

where G is called the processing gain.

2.1.1.2 Multiple-User Access

The second advantage of spread spectrum systems is the possibility of having multi-users on the same channel. Conventional transmission techniques split the channel

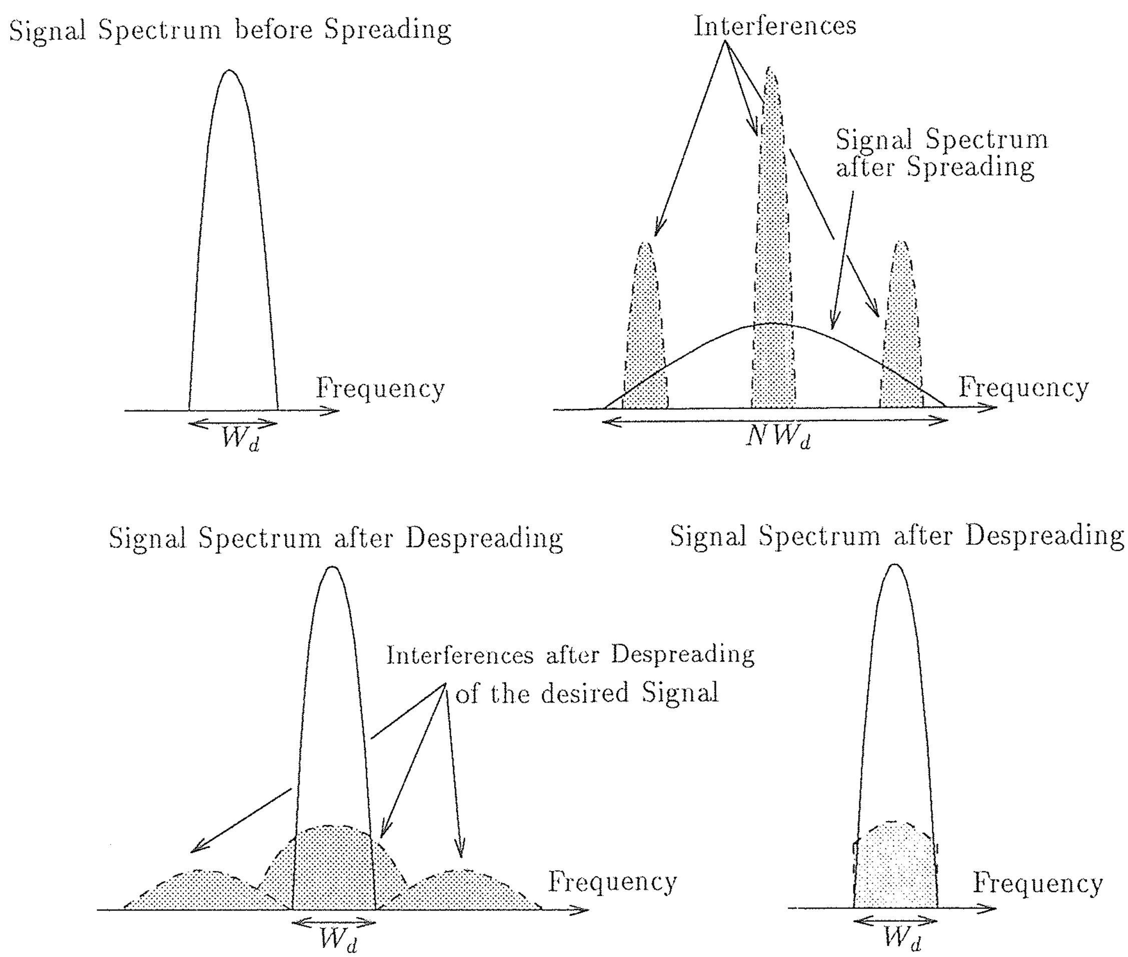

Figure 2.1 The Principal Steps in DSS Coders/Decoders

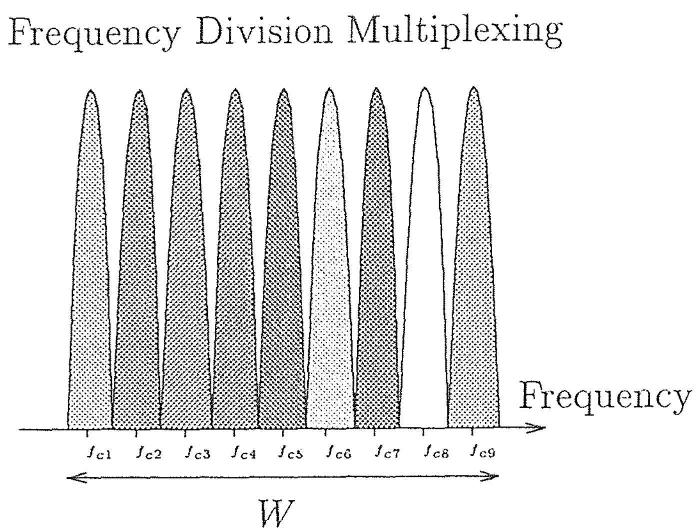

Figure 2.2 Different Multiplexing Techniques FDMA

into different time (TDMA) or frequency (FDMA) slots, Figures 2.2 and 2.3, respectively. These slots are assigned to specific users. In contrast, spread spectrum techniques assigns different codes to each of the users (which is CDMA), Figure 2.4, and allows them to use the whole bandwidth all the time. The way of achieving this is to spread the bits of each user with a different spreading sequence (code), where these codes must be orthogonal or semi-orthogonal to each other. In this way, either the users do not interfere with each other or only slightly decrease the performance of each other. This technique has the advantage that besides the multi-user feature, other problems such as fading or interference might be reduced.

2.2 Spreading Sequences

The heart of a spread spectrum system is the spreading sequence. The choice of this sequence will determine the performance of the system according to multiple access, jamming, intercept, fading channels and other properties. Therefore, a wide variety of sequences with different characteristics are available, and the system designer has

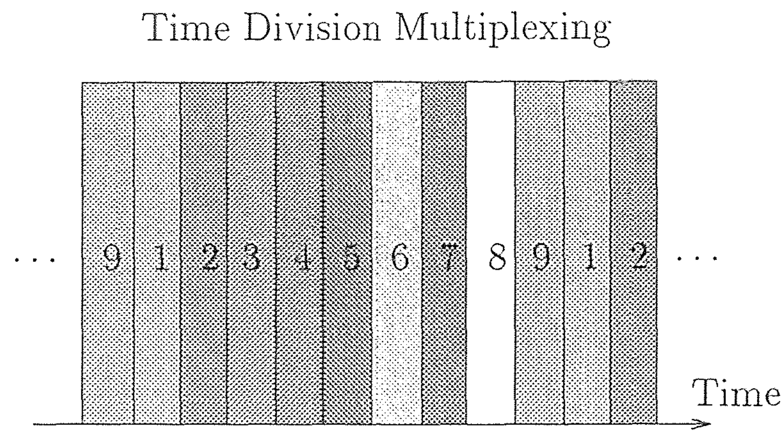

Figure 2.3 Different Multiplexing Techniques TDMA

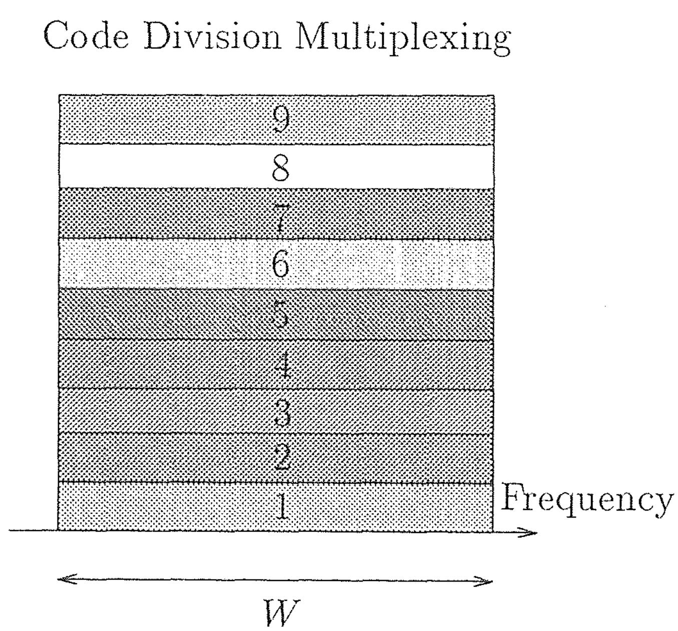

Figure 2.4 Different Multiplexing Techniques CDMA

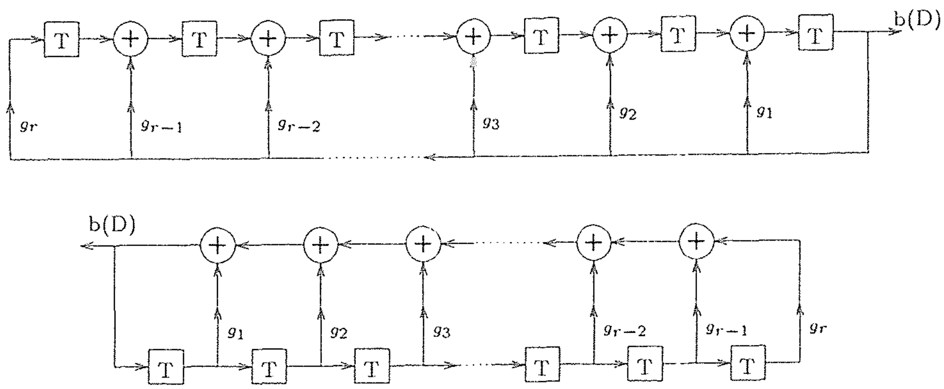

Figure 2.5 Typical m-Sequence Generators

a	b	$a+b$	ab
0	0	0	0
0	1	1	0
1	0	1	0
1	1	0	1
11	11	00	101

Table 2.1 Modulo-2 Arithmetic

to find the optimal sequence for the application at hand. In this chapter widely used sequences are evaluated and their performance in the DAB application are examined.

2.2.1 Maximal Length Sequences

The most common sequences for spreading are the maximal length sequences. Maximal length sequences are special sequences generated by recoupled shift registers (Fig. 2.5). The sequences generated by such a shift register are of maximal length if the feedback connections are chosen such that the shift register reaches any possible state, except the all zero-state, before repeating the sequence. The calculations required to generate PN-sequences require the use of modulo-2 arithmetic, where the operations shown in Table 2.1 are defined. Using these definitions, the mathematical description of such a generator polynomial is given as [25]

$$g(D) = 1 + g_1 D + g_2 D^2 + g_3 D^3 + \cdots + g_r D^r. \tag{2.4}$$

Here, the D-operator represents the unit delay, while the exponent refers a multiple of delay. The coefficients $\{g_i\}$ are either 1 or 0 and represent the feedback connections. The output $b(D)$ of such a generator is described by

$$b(D) = g_1 D b(D) + g_2 D^2 b(D) + g_3 D^3 b(D) + \cdots + g_r D^r b(D). \tag{2.5}$$

If the length of such a binary m-sequence is $N = 2^r - 1$, the maximal length, the polynomial is called a primitive polynomial. These primitive polynomials are of special importance, since the sequences generated by them have desired properties. The polynomials are given in their octal representation. For applications in a DAB-system, three of these properties are of special interest

1. In maximal length sequences, the number of ones is one more than the number of zeros. The number of ones in a sequence of length N is $\frac{1}{2}(N+1)$.

2. The periodic autocorrelation function $\Theta_b(k)$ of the sequence (Figure 2.8) is two-valued and is given by

$$\Theta_b(k) = \frac{1}{N}\sum_{n=0}^{N-1} a_n a'_{n+k} = \begin{cases} 1 & k = lN \\ -\frac{1}{N} & k \neq lN \end{cases} \quad l = 0, 1, 2, \cdots, \tag{2.6}$$

   where $a_n = (-1)^{b_n}$ as defined in [24].

3. The discrete Fourier transform of maximal length sequences is two-valued and constant for all non-zero frequencies (Figure 2.7).

Since the search for these m-sequences is difficult, generator polynomials are available in table forms [5, 15, 25]. The polynomials are given in their octal representations in those tables. The conversion into a binary number provides the coefficients for the generator polynomial g_i.

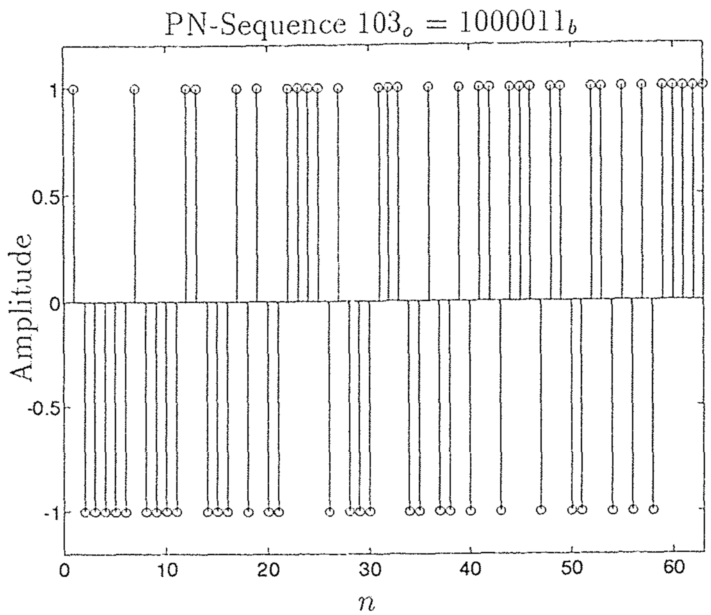

Figure 2.6 Typical m-Sequence

2.2.2 Gold Codes

The superb correlation and spectral properties of m-sequences come with the drawback of their limited varieties for a given length. This drawback is solved by using Gold codes. These sequences are available in large numbers, but their correlation properties are worse than those of m-sequences. Gold code generation starts with the choice of two preferred pairs of m-sequences of the desired length. Preferred pairs are chosen according to their cross-correlation properties and are available in table form [3, 4, 15]. The Gold code generator (see Figure 2.9) combines two m-sequences by modulo-2 addition of the outputs of their generators. This creates a single Gold code of length N. To generate different codes the output of one of m-generator is delayed. For each possible delay $1 \leq \tau \leq N$ we get a different Gold code. The overall number of possible Gold codes for a given pair of sequences is $N + 2$, since there are N different sequences corresponding to N delays, plus the two generator polynomials. The cross-correlation function of Gold codes has three

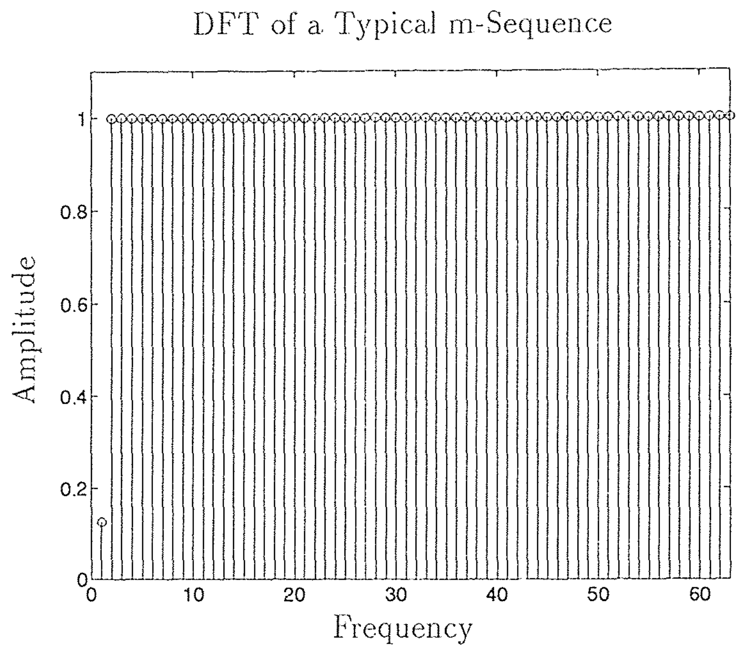

Figure 2.7 Fourier Transform of a Typical m-Sequence

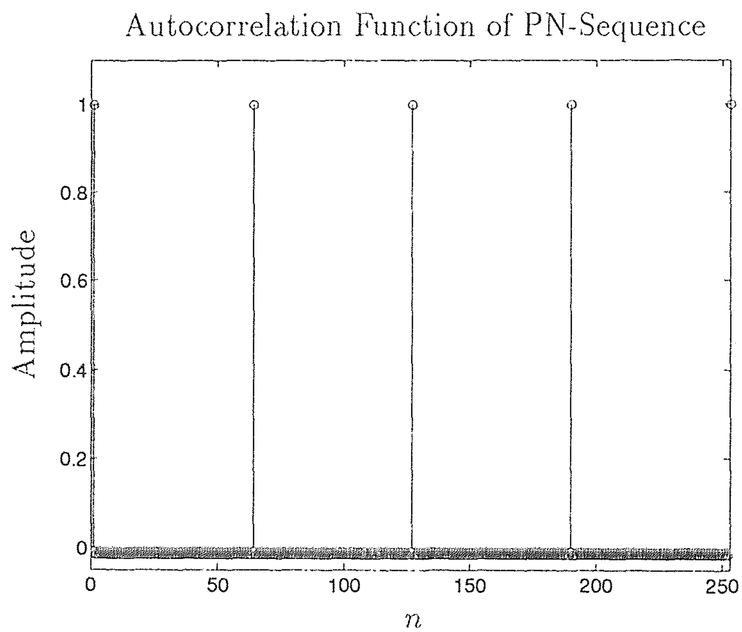

Figure 2.8 Autocorrelation Function of a Typical m-Sequence

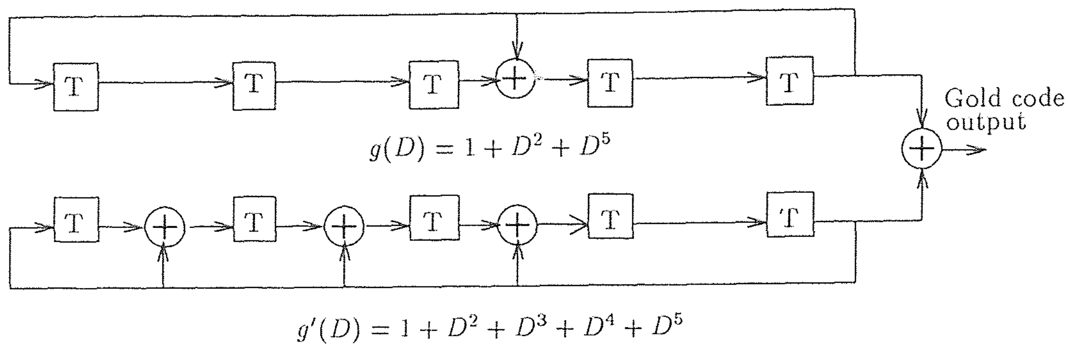

Figure 2.9 Typical Gold Code Generator

distinct values:

$$\Theta_{bb'} = \frac{1}{N}\sum_{n=0}^{N-1} a_n a'_{n+k} = \begin{cases} -\frac{1}{N}t(n) \\ -\frac{1}{N} \\ \frac{1}{N}[t(n)-2], \end{cases} \quad \text{where} \quad t(n) = \begin{cases} 1 + 2^{\frac{1}{2}(n+1)} & \text{for n odd} \\ 1 + 2^{\frac{1}{2}(n+2)} & \text{for n even.} \end{cases} \tag{2.7}$$

2.2.3 Walsh Codes

The last code mentioned here is the only orthogonal code in this group. The Walsh code has a zero cross-correlation, but its auto-correlation properties are worse than those of m-sequences and Gold codes. To generate these sequences, an iteration is performed which starts with the initial 2×2 Walsh matrix

$$A_0 = \begin{bmatrix} 1 & 1 \\ 1 & -1 \end{bmatrix}, \tag{2.8}$$

and grows an orthogonal matrix using the recursion,

$$A_{k+1} = \begin{bmatrix} A_k & A_k \\ A_k & -A_k \end{bmatrix}. \tag{2.9}$$

The iteration of Eq. (2.9) can be written in the form of the Kronecker Product of two matrices [2] as

$$A_{k+1} = A_0 \otimes A_k. \tag{2.10}$$

Walsh codes are of practical importance [21, 23] because of their cross-correlation properties. Since Walsh codes are orthogonal to each other, they have a zero cross-correlation. This property is useful for the synchronous transmission of multiuser data. For DAB, this property can be used to extend the data rate of the DSSS-system. Using Gold codes, the inter-user interference increases with the number of simultaneously transmitting users. This is because of the small but non-zero cross correlation between codes. Walsh codes do not cause any inter-user interference. Finally, it should be mentioned that Walsh codes have much higher sidelobes of their autocorrelation function. This can cause problems for multipath reception.

CHAPTER 3

DAB PROBLEM SCENARIOS

The newly developed Digital Audio Broadcasting technologies aim to fit the new digital data into the already occupied analog radio spectra. Therefore the new digital service is limited by already established analog audio broadcasting channels. Because of that, we review AM and FM transmission techniques in the following sections.

3.1 AM Channels

AM broadcasting is normally used today for low audio quality information services. The audio bandwidth for AM services is restricted to 5kHz, but some receivers may reduce this bandwidth even further. This is done to reduce noise and interference from neighboring channels. The RF bandwidth for AM transmission is restricted to 20kHz. The goal of a DAB system operating on AM channels is to provide a better digital audio quality within this narrow bandwidth, without disturbing the existing AM transmissions. In this section we present the fundamentals of AM transmission. Later we add a DAB-signal to it.

3.1.1 The AM Transmitter

The AM broadcasters transmit both sidebands and the carrier. This AM signal is generally generated by multiplying the message signal with the sinusoidal carrier. This can be written as [8]

$$s_{AM}(t) = A_c[1 + k_a m(t)] \cos(2\pi f_c t), \qquad (3.1)$$

where A_c is the carrier amplitude, f_c the carrier frequency, k_a the amplitude sensitivity and $m(t)$ the audio signal (message). For all of our calculations we assume

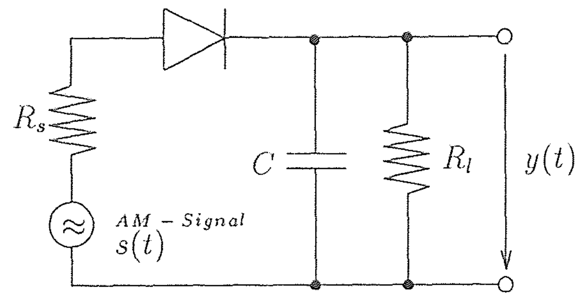

Figure 3.1 Envelope Detector

$|k_a m(t)| < 1$, for all t. The transmitter might mix this signal to the desired RF-frequency. Since the mixing operation is transparent to the signal, we will skip this and assume that it is performed without any significant error at both the transmitter and receiver side. The frequency domain representation of an AM signal is given as

$$S_{AM}(f) = A_c \frac{1}{2}\left[\delta(f - f_c) + \delta(f + f_c) + k_a M(f - f_c) + k_a M(f + f_c)\right], \qquad (3.2)$$

where $M(f)$ is the spectrum of the baseband message signal. The overall power of an AM signal is expressed as

$$P_{AM} = \frac{A_c^2}{2}(1 + k_a^2 P_m). \qquad (3.3)$$

3.1.2 The AM Receiver

For the demodulation of the received AM signal, there are two basic techniques available; coherent and noncoherent detection. We will first cover the two common noncoherent detection techniques, square law detection and envelope detection, before explaining coherent demodulation.

3.1.2.1 Envelope Detection

The simplest way of demodulating the AM signal is the envelope detector (Fig. 3.1). The envelope detector rectifies the received AM signal,

$$r(t) = s_{AM}(t) + n(t), \qquad (3.4)$$

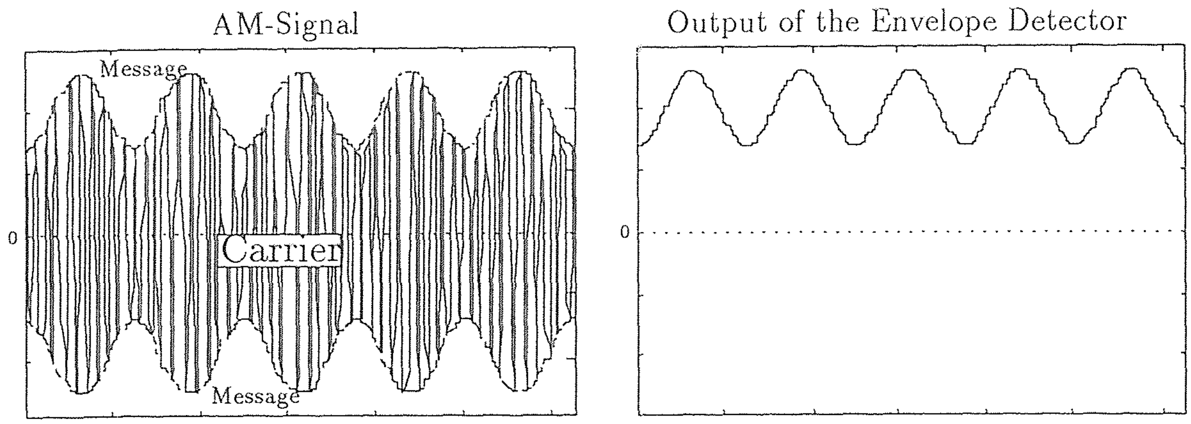

Figure 3.2 Input and Output of the Envelope Detector

where $n(t)$ is AWGN, and uses a low pass filter to recover the audio signal. The time constants in this realization (Fig. 3.1) have to be adjusted such that

$$R_s C \ll \frac{1}{f_c} \tag{3.5}$$

$$\frac{1}{f_c} \ll R_l C \ll \frac{1}{W}. \tag{3.6}$$

Here W is the bandwidth of the analog audio signal. In the ideal case, the mathematical description of the output signal of an envelope detector is given as

$$y(t) \simeq A_c[1 + k_a m(t)] + n_c(t), \tag{3.7}$$

where $n_c(t)$ is the in-phase component of narrow-band additive white Gaussian noise.

3.1.2.2 Square Law Detector

The second noncoherent demodulation technique, the square law detector, squares the incoming signal according to Equation (3.8) and uses a low pass filter of bandwidth W to recover the audio message

$$y(t) = a_1 s(t) + a_2 s^2(t). \tag{3.8}$$

The output of the squarer $y(t)$ can be rewritten as

$$y(t) = a_1 A_c[1+k_a m(t)]\cos(\omega_c t)+\frac{1}{2}a_2 A_c^2[1+2k_a m(t)+k_a^2 m^2(t)][1+\cos(2\omega_c t)]. \quad (3.9)$$

The desired signal $a_2 A_c^2 k_a m(t)$ is recovered at the output of with a low pass filter. The energy of $a_2 A_c^2 k_a^2 m^2(t)$ within the message bandwidth W is negligible if $|k_a m(t)| \ll 1$ for all t.

3.1.2.3 Coherent Demodulation

The coherent demodulation of an AM signal requires the receiver to recover the carrier out of the incoming signal. To demodulate the message, the incoming signal is multiplied by a sinusoid

$$r(t) = A_c[1 + k_a m(t)]\cos(2\pi f_c t)\frac{2}{A_c k_a}\cos(2\pi f_c t + \theta_{LO}), \quad (3.10)$$

where $\frac{2}{A_c k_a}$ is the amplitude of the local oscillator. This value is chosen for convenience. θ_{LO} is the phase error of the local oscillator. Therefore, the output signal of the receiver, after filtering out the high frequency components $\cos(4\pi f_c t + \theta_{LO})$, is found as

$$v(t) = [\frac{1}{k_a} + m(t)]\cos(\theta_{LO}). \quad (3.11)$$

The $\cos(\theta_{LO})$ term must be equal to one for perfect recovery. But for all small angles of θ_{LO} the message is demodulated in a satisfactory manner. The DC term is filtered out by using a capacitor coupling.

3.2 FM Channels

Audio broadcasting for entertainment today is almost completely done by using FM. This is the consequence of the better audio quality of frequency modulated broadcasts than AM. The standard for FM audio broadcasting restricts the bandwidth of the

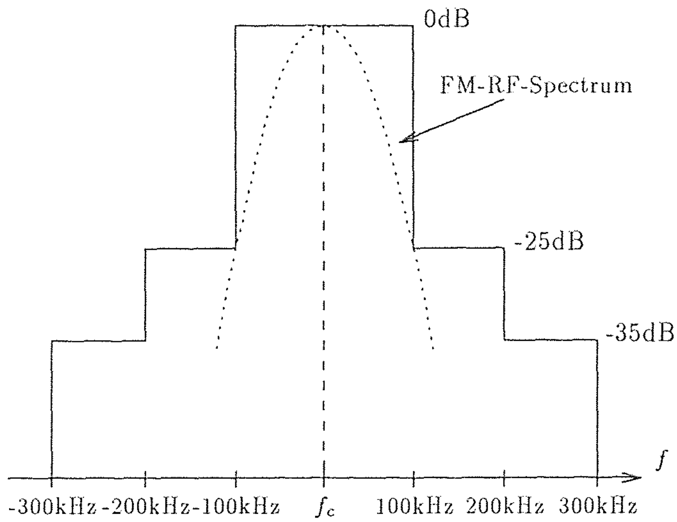

Figure 3.3 FCC-FM Channel Mask

analog audio signal to 15kHz, while the RF bandwidth is regulated using the FCC-FM-mask, [Fig. 3.3]. In this section, we will revisit the fundamentals of FM communications systems.

3.2.1 FM Transmitter

The FM transmitter changes the instantaneous frequency of its sinusoidal carrier f_c according to the message $m(t)$ as

$$f_i(t) = f_c + k_f m(t), \tag{3.12}$$

where k_f is the frequency sensitivity of the modulator. If we integrate Equation (3.12) with respect to time t and multiply by 2π we get the angle of the carrier,

$$\Theta_i(t) = 2\pi f_c t + 2\pi k_f \int_0^t m(t)\,dt, \tag{3.13}$$

where we assume that for $t = 0$ the unmodulated carrier has a zero phase. Therefore, the FM signal in time domain is given as

$$s_{FM}(t) = A_c \cos\left[2\pi f_c t + 2\pi k_f \int_0^t m(t)\,dt\right]. \tag{3.14}$$

For a single tone message $m(t) = A_m \cos(2\pi f_m t)$, the instantaneous frequency $f_i(t)$ is shown as

$$f_i(t) = f_c + k_f A_m \cos(2\pi f_m t) \quad (3.15)$$

$$= f_c + \Delta f \cos(2\pi f_m t), \quad (3.16)$$

where $\Delta f = k_f A_m$ is the frequency deviation. The frequency deviation represents the maximal departure of the instantaneous frequency from the carrier frequency. If we define the modulation index β as

$$\beta = \frac{\Delta f}{f_m}, \quad (3.17)$$

we can write the FM signal for a single tone message as

$$s(t) = A_c cos[2\pi f_c t + \beta \sin(2\pi f_m t)], \quad (3.18)$$

where β represents the phase deviation of the FM wave from the unmodulated carrier.

To calculate the frequency domain representation of the FM-signal, we have to write it in the form of its complex envelope

$$s_{FM}(t) = Re[\tilde{s}(t) e^{j2\pi f_c t}], \quad (3.19)$$

where $\tilde{s}$ is the complex envelope of the FM-signal,

$$\tilde{s}(t) = A_c e^{j\beta \sin(2\pi f_m t)}, \quad (3.20)$$

and expressed in a complex Fourier series as

$$\tilde{s}(t) = \sum_{n=-\infty}^{\infty} c_n e^{2\pi n f_m t}, \quad (3.21)$$

where the complex Fourier coefficients $\{c_n\}$ are defined as

$$c_n = \int_{-\frac{1}{2} f_m}^{\frac{1}{2} f_m} \tilde{s}(t) e^{-2\pi n f_m t} \, dt \quad (3.22)$$

$$= f_m A_c \int_{-\frac{1}{2} f_m}^{\frac{1}{2} f_m} e^{j\beta \sin(2\pi f_m t) - j2\pi n f_m t} \, dt. \quad (3.23)$$

For $x = 2\pi f_m t$, this integral has the form of the n^{th} order Bessel function of the first kind and argument β, $J_n(\beta)$,

$$J_n(\beta) = \frac{1}{2\pi}\int_{-\pi}^{\pi} e^{j(\beta\sin(x)-nx)}\,dt. \tag{3.24}$$

Some of the Bessel functions are plotted in Figure 3.4. The coefficients are expressed as $c_n = A_c J_n(\beta)$. Using the Bessel Functions we can rewrite equation (3.19) as follows

$$\begin{aligned} s_{FM}(t) &= A_c Re\left[\sum_{n=-\infty}^{\infty} J_n(\beta) e^{j2\pi(f_c+nf_m)t}\right] && (3.25)\\ &= A_c \sum_{n=-\infty}^{\infty} J_n(\beta) cos(j2\pi(f_c+nf_m)t). && (3.26)\\ & && (3.27)\end{aligned}$$

Hence the Fourier transform of this signal is found as

$$S_{FM}(f) = \frac{A_c}{2}\sum_{n=-\infty}^{\infty} J_n(\beta)\left[\delta(f-f_c-nf_m)+\delta(f+f_c+nf_m)\right]. \tag{3.28}$$

3.2.2 FM Receiver

The FM receiver has to recover the audio data from the received frequency modulated signal. Therefore, it is necessary to have a circuit that changes the amplitude linearly with the frequency around the carrier. The most common demodulator is the PLL demodulator. The PLL demodulator tracks the changes of the signal frequency and produces an output voltage proportional to the frequency change necessary to track the signal.

3.2.2.1 The PLL

The PLL is a negative feedback control circuit. The main components of a PLL circuit are shown in Figure 3.5. For our calculations it is important that the VCO is adjusted such that the output frequency for zero input is exactly the carrier

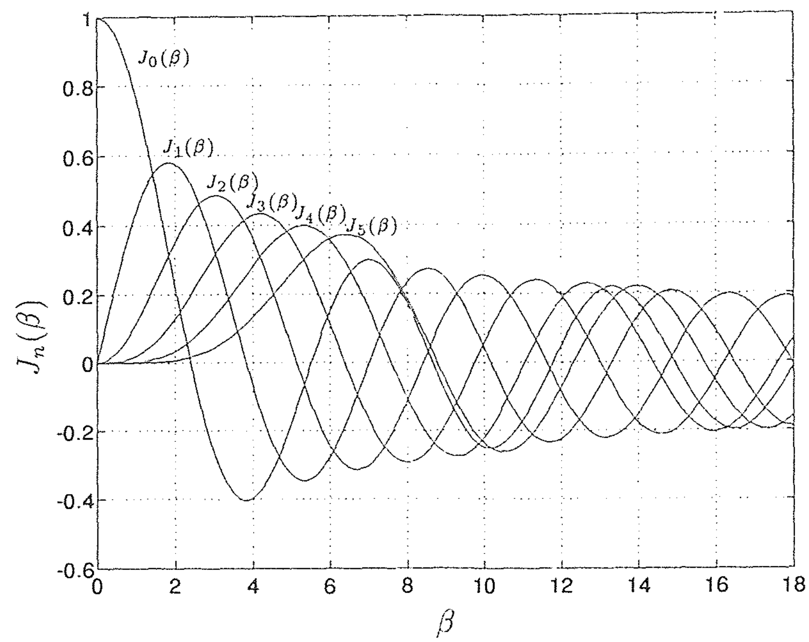

Figure 3.4 Bessel Function of the First Kind

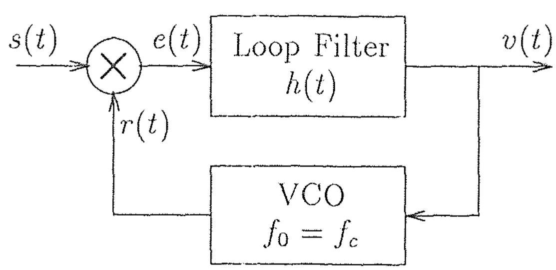

Figure 3.5 Main Components of a PLL

frequency of the FM signal with a phase shift of $\frac{\pi}{2}$. The FM signal $s(t)$ can be written as

$$s(t) = A_c \sin\left[2\pi f_c t + \phi_1(t)\right], \tag{3.29}$$

where the Sine function is due to the phase shift of $\frac{\pi}{2}$ and

$$\phi_1(t) = 2\pi k_f \int_0^t m(t)\, dt. \tag{3.30}$$

The output signal of the VCO, $r(t)$, is found as

$$r(t) = A_v \cos\left[2\pi f_c t + \phi_2(t)\right], \tag{3.31}$$

where

$$\phi_2(t) = 2\pi k_v \int_0^t v(t)\, dt, \tag{3.32}$$

and A_v is the amplitude of the VCO output signal. The constant k_v is the frequency sensitivity of the VCO. The output of the multiplier $e(t)$ can be written as

$$\begin{aligned} e(t) &= A_c A_v \sin\left[2\pi f_c t + \phi_1(t)\right] \cos\left[2\pi f_c t + \phi_2(t)\right] && (3.33)\\ &= \frac{A_c A_v}{2}\left[\sin\left(\phi_1(t) - \phi_2(t)\right) + \sin\left(4\pi f_c t + \phi_1(t) + \phi_2(t)\right)\right]. && (3.34)\end{aligned}$$

Defining

$$\phi_e(t) = \phi_1(t) - \phi_2(t), \tag{3.35}$$

the output of the loop filter $v(t)$ can be written as

$$\begin{aligned} v(t) &= \int_{-\infty}^{\infty} e(\tau) h(t-\tau)\, d\tau, && (3.36)\\ &= \int_{-\infty}^{\infty} \frac{A_c A_v}{2}\left[\sin\left(\phi_e(t)\right) h(t-\tau)\, d\tau\right] + 0. && (3.37)\end{aligned}$$

Recognizing that $\phi_e(t)$ can be written as

$$\phi_e(t) = \phi_1(t) - 2\pi k_v \int_0^t v(t)\, dt, \tag{3.38}$$

taking the first derivative with respect to t and replacing $v(t)$ with Eq. (3.37) gives

$$\frac{d\,\phi_e(t)}{dt} = \frac{d\,\phi_1(t)}{dt} - 2\pi K_0 \int_{-\infty}^{\infty} \sin\left(\phi_e(t)\right) h(t-\tau)\, d\tau. \tag{3.39}$$

In Eq. (3.39), the constant $K_0 = \frac{2\pi A_v A_c}{2}$. If the phase error $\phi_e(t)$ is equal to zero, the PLL is said to be in phase lock. In this operation mode, we can simplify the system by replacing

$$\sin(\phi_e(t)) \approx \phi_e(t), \quad \text{since,} \quad \phi_e(t) \ll 1\,rad. \tag{3.40}$$

Now we can write a linear model for the PLL circuit as

$$\frac{d\,\phi_e(t)}{dt} + 2\pi K_0 \int_{-\infty}^{\infty} \phi_e(t)h(t-\tau)\,d\tau = \frac{d\,\phi_1(t)}{dt}. \tag{3.41}$$

Taking the Fourier Transform of Eq. (3.41), we can write

$$\Phi_e(f) = \frac{\Phi_1(f)}{1 + \frac{K_0 H(f)}{jf}}. \tag{3.42}$$

Introducing the loop transfer function $L(f)$ as

$$L(f) = \frac{K_0 H(f)}{jf}, \tag{3.43}$$

we are able to rewrite $\Phi_e(f)$ as

$$\Phi_e(f) = \frac{\Phi_1(f)}{1 + L(f)}. \tag{3.44}$$

In this equation, we see that $\Phi_e(f) \to 0$ for $|L(f)| \gg 1$. Rewriting the output $V(f)$ in terms of $\Phi_e(f)$ results in

$$V(f) = \frac{jf}{k_v} L(f)\Phi_e(f). \tag{3.45}$$

Substituting $\Phi_e(f)$ by its equivalent in Eq. (3.44),

$$V(f) = \frac{\frac{jf}{k_v} L(f)}{1 + L(f)}\Phi_1(f). \tag{3.46}$$

This can be approximated for $|L(f)| \gg 1$ by

$$V(f) \approx \frac{jf}{k_v}\Phi_1(f). \tag{3.47}$$

In the time domain, Eq. (3.47) can be written as

$$v(t) \approx \frac{1}{2\pi k_v}\frac{d\,\phi_1(t)}{dt}. \tag{3.48}$$

Thus, provided that $|L(f)| \gg 1$ for all frequencies of interest, we may model the PLL as a differentiator with the input scaled by $\frac{1}{2\pi k_v}$. Therefore, the PLL demodulator for FM signals can be written as

$$v(t) \approx \frac{k_f}{k_v} m(t), \tag{3.49}$$

where we substituted Eq. (3.30) into Eq. (3.48).

3.3 Digital Modulation Techniques

3.3.1 Binary Phase Shift Keying

Binary phase shift keying (BPSK) is a common, simple form of modulation used for the transmission of digital signals [16]. In binary phase shift keying the carrier is shifted in phase according to the data signal. Hereby the phase is able to take on two distinct values separated by a phase difference of $\Delta\Theta = \pi$. For a transmitted power of $P_s = 0.5A_c^2$, the BPSK signal can be written either as

$$\begin{aligned} s_{BPSK1}(t) &= \sqrt{2P_s}\cos(\omega_c t) \\ \text{or } s_{BPSK2}(t) &= \sqrt{2P_s}\cos(\omega_c t + \pi) \\ &= -\sqrt{2P_s}\cos(\omega_c t). \end{aligned} \tag{3.50}$$

If we convert the digital data stream $d(t)$ into a bipolar signal, which can take on either 1 or -1 values, we can write the BPSK signal as

$$s_{BPSK}(t) = d(t)\sqrt{2P_s}\cos(\omega_c t). \tag{3.51}$$

At the receiver side, the carrier has to be recovered without any significant phase error. Then, the demodulation is done by using synchronous demodulation and an integrate-and-dump circuit. The output of the synchronous demodulator in the absence of noise is given by

$$c(t) = d(t)\sqrt{2P_s}\cos^2(\omega_c t + \Theta_{channel}), \tag{3.52}$$

where $\Theta_{channel}$ is the phase shift caused by the run-time delay of the transmission channel. This signal is fed into the integrator that is controlled by a bit synchronizer.

Then the signal $c(t)$ is integrated over one bit period T_d. For the k^{th} bit the output signal $y(kT_d)$ is expressed as

$$y(kT_d) = d(kT_d)\sqrt{2P_s}\int_{(k-1)T_d}^{kT_d} \cos^2(\omega_c t + \Theta_{channel})dt. \tag{3.53}$$

If we choose the carrier frequency to be an integer multiple of the bit period, that is, $\omega_c = 2\pi n \frac{1}{T_d}$, then the integration for the Sine component over one bit is zero and the output is found as

$$y(kT_d) = d(kT_d)\sqrt{\frac{P_s}{2}}T_d. \tag{3.54}$$

3.3.1.1 Power Spectral Density of BPSK Signals

The data waveform $b(t)$ is an NRZ binary waveform whose power spectral density is given by

$$G_d(f) = P_s T_d \left(\frac{\sin \pi f T_d}{\pi f T_d}\right)^2. \tag{3.55}$$

The BPSK-signal (Eq. 3.51) convolves this signal $G_d(f)$ with the δ-function located at $\delta(f \pm f_c)$ (cosine modulation). Therefore, the PSD function of a BPSK signals is expressed as [16]

$$G_d(f) = \frac{P_s T_d}{2}\left\{\left[\frac{\sin \pi(f-f_c)T_d}{\pi(f-f_c)T_d}\right]^2 + \left[\frac{\sin \pi(f-f_c)T_d}{\pi(f-f_c)T_d}\right]^2\right\}. \tag{3.56}$$

3.3.1.2 Geometric Interpretation of a BPSK Signal

We can represent the BPSK-signal, Eq. (3.51), as an orthonormal signal $u_1(t) = \sqrt{\frac{2}{T_d}}\cos(\omega_c t)$. Therefore, we can write

$$s_{BPSK}(t) = \sqrt{P_s T_d}d(t)\sqrt{\frac{2}{T_d}}\cos(w_c t). \tag{3.57}$$

The distance between the BPSK signal points is found as

$$d = 2\sqrt{P_s T_d} = 2\sqrt{E_d}, \tag{3.58}$$

where $E_d = P_s T_d$ is the energy per bit.

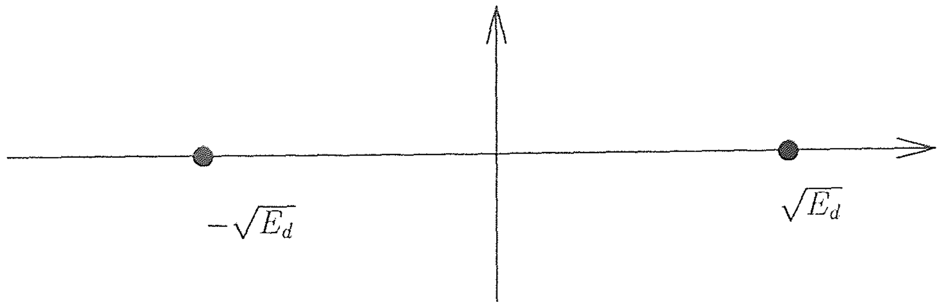

Figure 3.6 Geometric Representation of a BPSK Signal

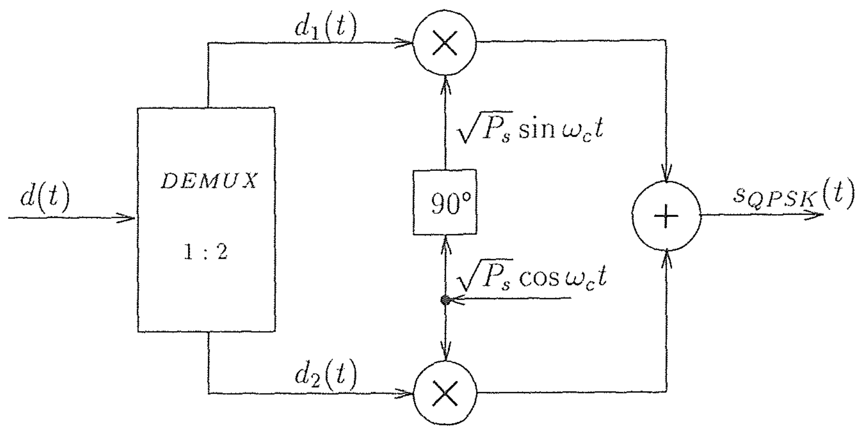

Figure 3.7 QPSK System Block Diagram

3.3.2 Quadrature Phase Shift Keying

We have seen that the bandwidth of the BPSK signal is $B_{BPSK} = \frac{1}{2T_d}$. This means that we need two hertz of bandwidth to transmit a single bit per second. One way of reducing this bandwidth is not to use only two phase values, but, e.g., four distinct phases to transmit the bit stream, which is QPSK modulation. In QPSK modulation the bit stream is split into two equal data rate streams (Fig. 3.7). These data streams are BPSK-coded with a phase shift of $\frac{\pi}{2}$ to each other. Then both BPSK signals are added and transmitted. The mathematical description of this system is as follows

$$
\begin{aligned}
s_{QPSK}(t) &= \sqrt{P_s} d_1(t) \cos(\omega_c t) d_2(t) \sin(\omega_c t) \\
&= \sqrt{P_s} \cos(\omega_c t + \theta_1(t)) \sin(\omega_c t + \theta_2(t)) \qquad (3.59)
\end{aligned}
$$

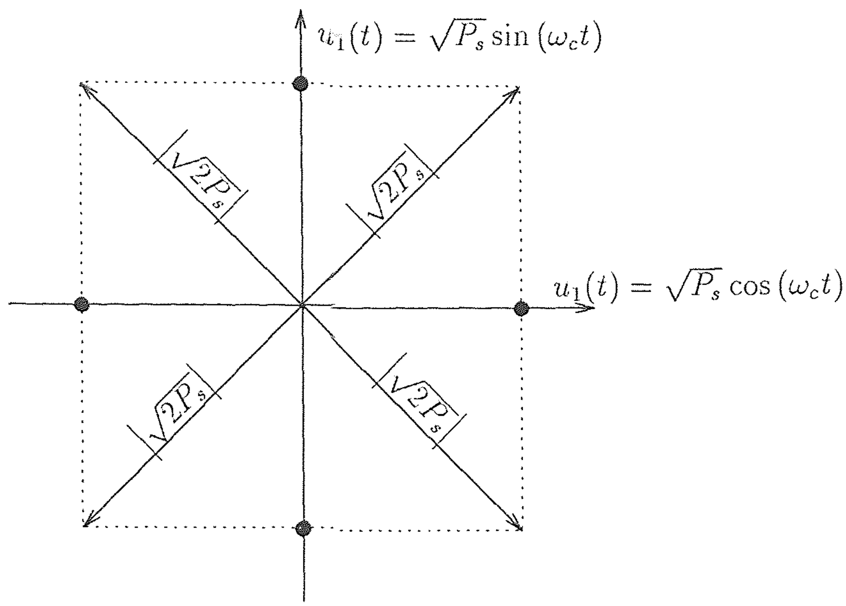

Figure 3.8 QPSK Geometrical Interpretation

$$
\begin{aligned}
&= \sqrt{P_s}\left[2\cos\left(\omega_c t + \frac{\theta_1(t)+\theta_2(t)}{2} - \frac{\pi}{4}\right)\cos\left(\frac{\theta_1(t)-\theta_2(t)}{2} + \frac{\pi}{4}\right)\right] \\
&= \sqrt{2P_s}\cos\left(\omega_c t + \theta_{QPSK}(t)\right),
\end{aligned}
$$

where

$$
\theta_{QPSK}(t) \in \left\{\frac{\pi}{4}; \frac{3\pi}{4}; -\frac{3\pi}{4}; -\frac{\pi}{4}\right\}. \tag{3.60}
$$

The power spectral density of this signal is equal to that of a BPSK signal with half the bit rate. Therefore, the bandwidth needed to transmit a single bit per second is reduced to one hertz.

The QPSK as seen above can be interpreted as a sinusoid with a four-valued distinct phase for each of the four symbols [Fig. 3.8].

CHAPTER 4

VARIOUS FREQUENCY EXCISERS

4.1 Transform Domain-Based Excisers

Linear block transforms are widely used for engineering applications. The DCT is the international decomposition standard for audio and video compression. The DFT is the most common transform for signal processing applications. In contrast to these fixed transforms, the KLT makes use of the statistical properties of the signal. It is the optimal decomposition of a signal for a given square transform size and signal statistics. The frequency behavior of block transforms is restricted by the transform size. All block transforms suffer from the limited time-frequency localization of their transform bases. Filter banks or subband transforms overcome this drawback. The length of the transform basis (filters) can be chosen independent from the number of subbands or basis functions. Therefore, fine tuning of the transformation filters (basis) according to the special needs of the application is possible [17, 18, 20]. Recently, it is well recognized that the block transforms and subband transforms are only special cases of the Generalized Linear Transforms (GLT).

4.1.1 Introduction to Generalized Linear Transforms

The maximally decimated regular M-band PR-QMF structure, shown in Figure 4.1, decompose the signal into M equal bandwidth subbands. The anti-aliasing filters $\{h_r(k)\}$ reduce the bandwidth to $\frac{\pi}{M}$ wide subbands. Therefore, decimation by a factor of M is justified. In case of no intermediate processing, the upsampling by M and interpolation with $\{g_r(k)\}$ perfectly recovers the input signal with a delay. In this case the set of filters $\{h_r(k)\}$ and $\{g_r(k)\}$ are said to be perfect reconstruction. This PR-condition property requires a stable and paraunitary transform matrix

$\mathbf{H}(z)$, such that

$$\tilde{\mathbf{H}}(z)\mathbf{H}(z) = d\mathbf{I} \tag{4.1}$$

where d is some delay and $\mathbf{I}$ the identity matrix. $\tilde{\mathbf{H}}(z)$ is the paraconjugate of $\mathbf{H}(z)$. The paraconjugate matrix is defined in [2, 22] as

$$\tilde{\mathbf{H}}(z) = \mathbf{H}^H(z^{-1}), \tag{4.2}$$

where $\mathbf{H}^H$ is the hermitian or conjugate transposed of $\mathbf{H}$. This paraunitary condition forces the analysis filters to satisfy the conditions

$$\sum_k |h_r(k)|^2 = 1 \tag{4.3}$$

$$\sum_k h_r(k)h_r(k + Mn) = 0 \quad \text{for} \quad n \neq 0 \tag{4.4}$$

$$\sum_k h_r(k)h_s(k + Mn) = 0 \quad \text{for} \quad \forall n, \tag{4.5}$$

where $\{h_r(k)\}$ are the analysis filters and $M \neq 0$. The synthesis filters $\{g_r(k)\}$ are obtained from the analysis filters in a paraunitary system defined as

$$g_r(k) = h_r(N - 1 - k), \tag{4.6}$$

where N is the length of the filter. In case of block transforms, the conditions of Eqs.(4.3) - (4.5) reduce to

$$\sum_k |h_r(k)|^2 = 1 \tag{4.7}$$

$$\sum_k h_r(k)h_s(k) = 0, \tag{4.8}$$

since $\mathbf{H}(z)$ is a square matrix of size $M \times M$.

A different implementation of the maximally decimated equal M-band PR-QMF structure can be achieved by reusing the same split for decomposing the subband signals again. For a 2-band PR-QMF filter bank a regular hierarchical tree is shown in Figure 4.2. The design of such a tree is much easier than that of the M-band direct structure. In addition to that, the module structure simplifies

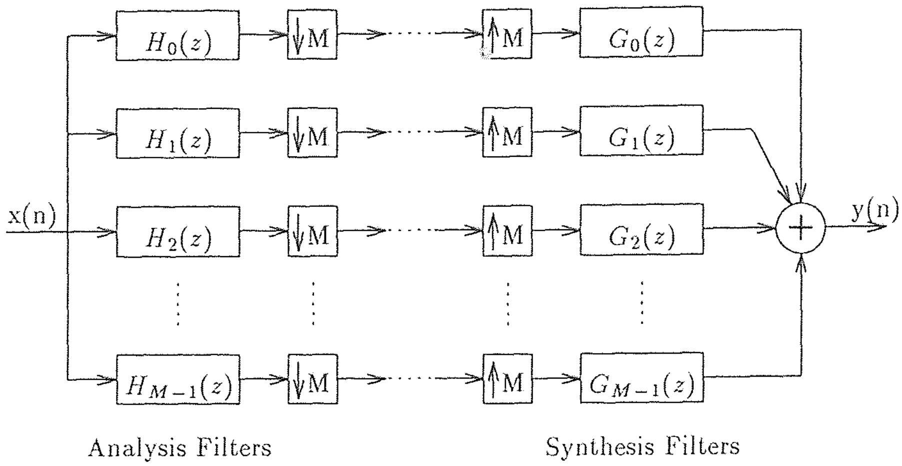

Figure 4.1 Maximally Decimated Equal M-Band PR-QMF Structure

the implementation. But as the number of levels increases, the aliasing in between subbands becomes more significant. To process signals with different resolutions, the dyadic tree (Fig. 4.3) can be used. Each additional level adds more details to the signal, such that the original resolution is reached when all subbands are used. This tree structure is widely used in multirate signal processing, such as video coding.

The irregular tree, shown in Figure 4.4 is the most flexible structure. According to the special design requirements each level can use different filters and splits. For a given, fixed signal characteristic this tree structure is able to perform an optimal decomposition, fitting all spectral constraints.

4.1.2 Regular Subband Exciser

The regular tree subband structures (Fig. 4.2) can be used as a frequency exciser [12]. The received signal is decomposed into M equal bandwidth subbands. These subbands are checked for their energy contents. Thereby, the subbands containing significant amount of interference will have the highest energy levels. These subbands are discarded and the synthesis stage recovers the excised signal. The use of equal bandwidth subbands is required for this application. Since the exact locations of

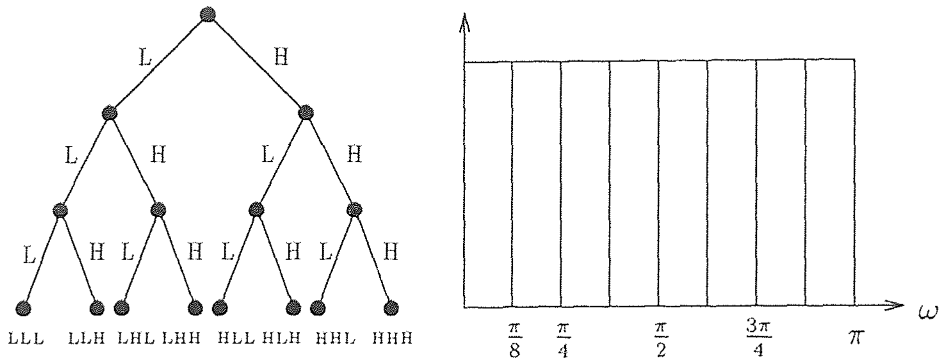

Figure 4.2 A Regular Subband Tree and Equal Bandwidth 8-Band Spectrum

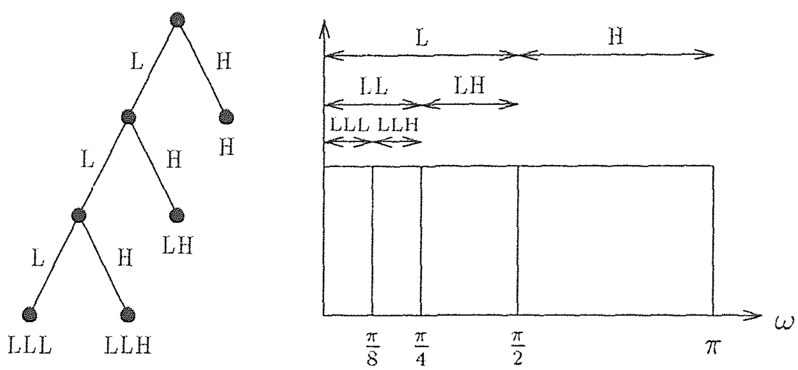

Figure 4.3 A Dyadic Subband Tree and Unequal Bandwidth 4-Band Spectrum

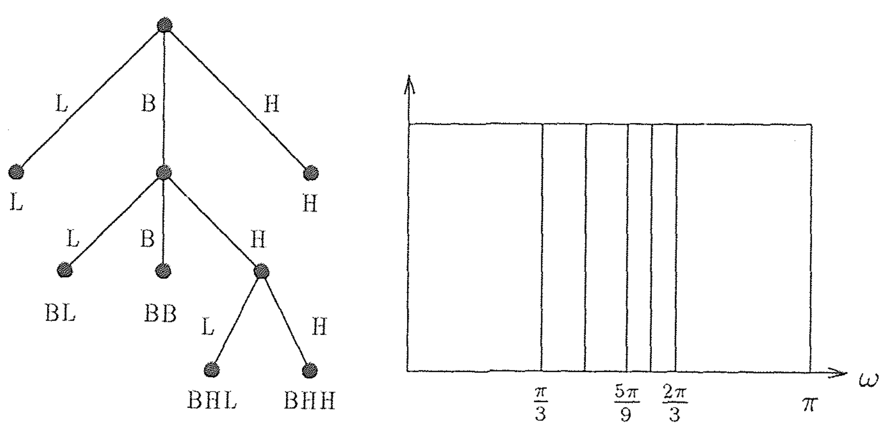

Figure 4.4 An Irregular Subband Tree and Unequal Bandwidth 6-Band Spectrum

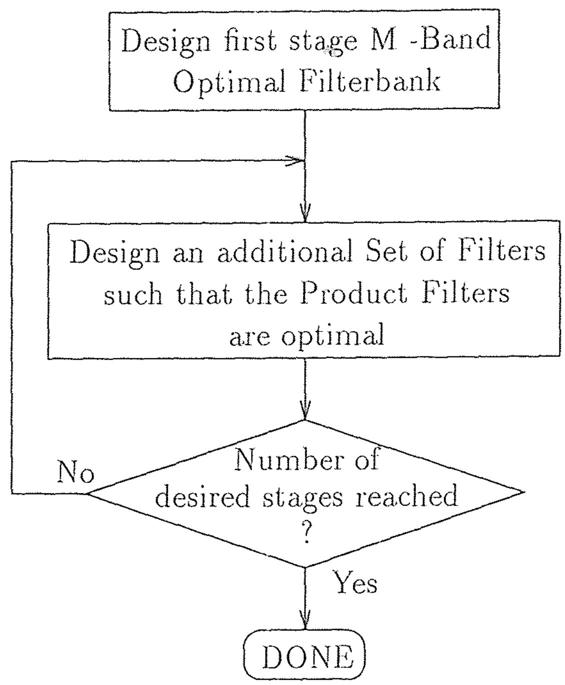

Figure 4.5 The Progressive Optimization Algorithm [18]

interferences is unknown, all possible bands have to be treated equally to ensure constant performance for all frequency location of interferences.

Designing such filterbanks can be done by searching for a prototype, e.g. 2-band PR-QMF filter, and reusing it according to the desired tree-structure. Better performance can be achieved by designing the tree using the progressive optimization technique [18]. This technique assures the best performance for tree structured filterbanks. The design algorithm is illustrated in Figure 4.5. The first step designs an optimal set of filters for the first stage of the desired tree structure. The next step searches for the second stage filters of the tree such that the product filters are optimal under the design constrains. This step is repeated until the desired number of stages reached. The product filters for a filterbank can be calculated as follows, for Figure 4.6,

$$H_L(z) = H_L(z)$$

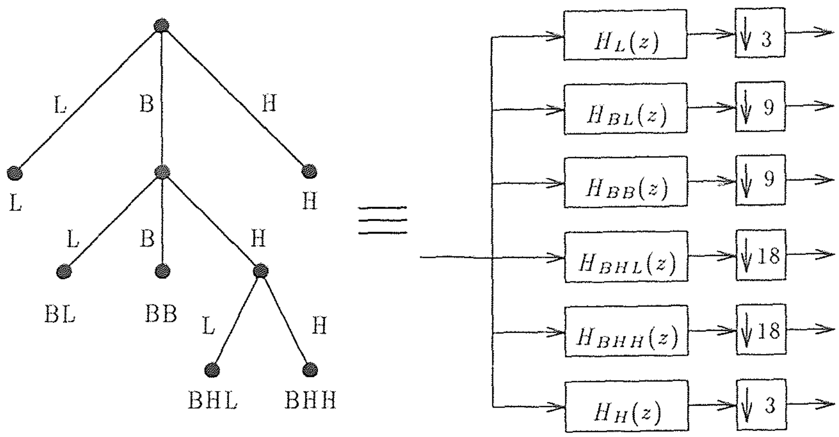

Figure 4.6 Equivalent Direct Structure of Product Filters

$$
\begin{aligned}
H_{BL}(z) &= H_B(z)H_L(z^3) \\
H_{BB}(z) &= H_B(z)H_B(z^3) \\
H_{BHL}(z) &= H_B(z)H_H(z^3)H_L(z^9) \\
H_{BHH}(z) &= H_B(z)H_H(z^3)H_H(z^9) \\
H_H(z) &= H_H(z)
\end{aligned}
\tag{4.9}
$$

In case of the 64-band filterbank (Figure 4.7), three sets of 4-band filters were designed [18]. The 64 product filters were calculated and used for a direct structure implementation of the filterbank. In Figure 4.7 it can be seen, that the aliasing in between different subbands causes the filterbank to perform differently for different frequency locations. This frequency behavior was studied in [17, 19].

4.1.3 Adaptive Subband Exciser

The tree structures mentioned before have one major drawback; once they are designed, their properties are fixed. This is of special concern for the excision of interferences, as in DAB. There the localizations of the interferences are changing with the FM-modulated analog signal. The performance of fixed based excisers are depending on the frequency location of the interference, as shown in [17, 19]. Therefore, a fixed

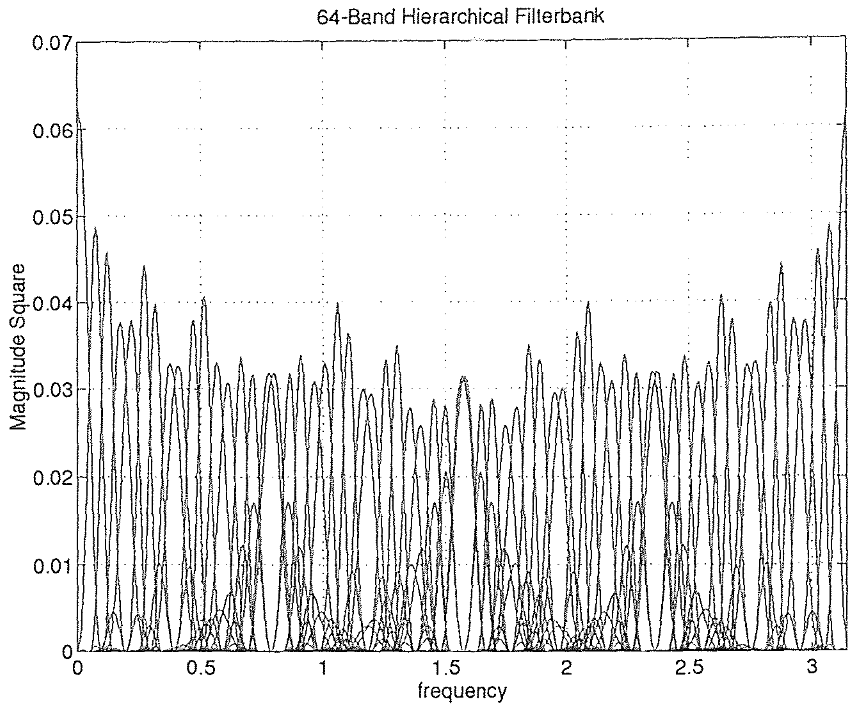

Figure 4.7 64-Band Filterbank Frequency Response

transform can not perform well. The excision of the FM-interferences requires the adaptation of a decomposition structure to the spectral unevenness of the signal. This can be done, since the data-signal is a wide band signal spreaded in frequency, while the interference is localized in frequency. Therefore, evaluating the spectral unevenness of the received signal will localize the interference.

One common measure for the spectral unevenness is the energy compaction of a transform [2]

$$G = \frac{\sigma_x^2}{\left[\prod_{i=1}^{M} \sigma_i^2\right]^{1/M}}, \tag{4.10}$$

where σ_x^2 is the input variance and $\{\sigma_i^2\}$ are the subband variances. The adaptive frequency exciser utilizes an adaptive subband transform based on a tree structuring algorithm [1, 17, 19]. The tree structuring algorithm checks the spectral unevenness of the incoming signal for two possible splits, the 2- or 3-band decompositions. This

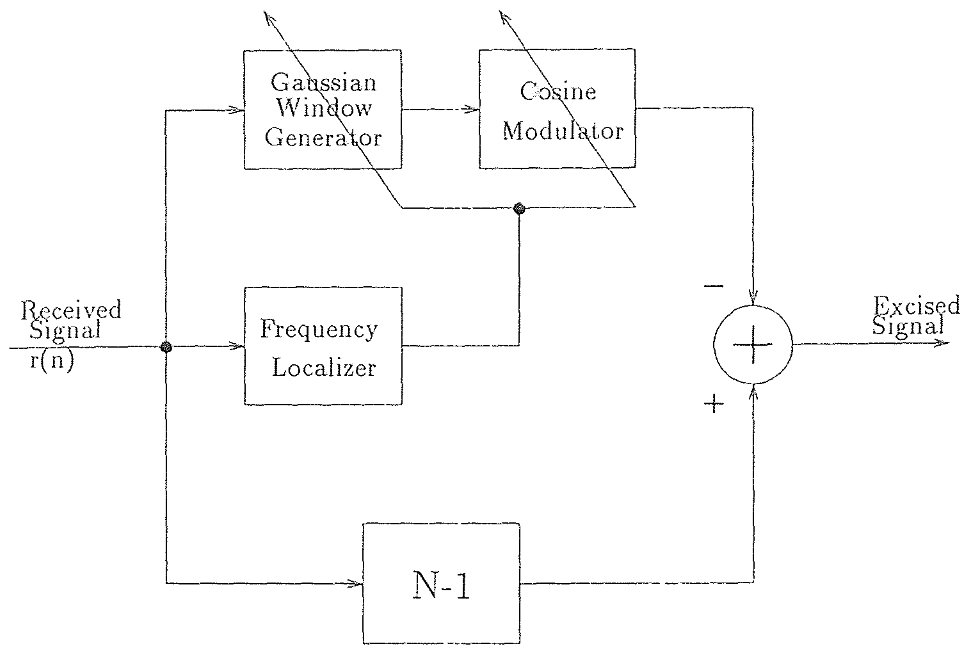

Figure 4.8 General Structure of a Window Exciser

treatment overcomes the problems accompanied by interferences in the transition regions of the filters, at $\frac{\pi}{2}$, $\frac{\pi}{3}$ or $\frac{2\pi}{3}$. If one of the compaction measures exceeds a predefined threshold T, decomposition is performed. To narrow the bandwidth of the subbands down to the interference, the subband variances are calculated and the interfered subband with the highest power level is further decomposed. Finally, a desired frequency resolution is reached. Then, the subband which contains the interference is excised and the synthesis of the remaining subbands is performed [2, 22].

4.2 Sliding and Variable Binomial-Gaussian Window-Based Exciser

Beside the adaptive subband exciser a second technique of excising interferences is the use of a sliding and variable frequency window [13]. This window adapts its bandwidth and frequency location to the exact bandwidth and center frequency of the interferences. Therefore, it can be used to extract the interferences out of the spectrum. Because of its simplicity and applicability, we use the Binomial-Gaussian

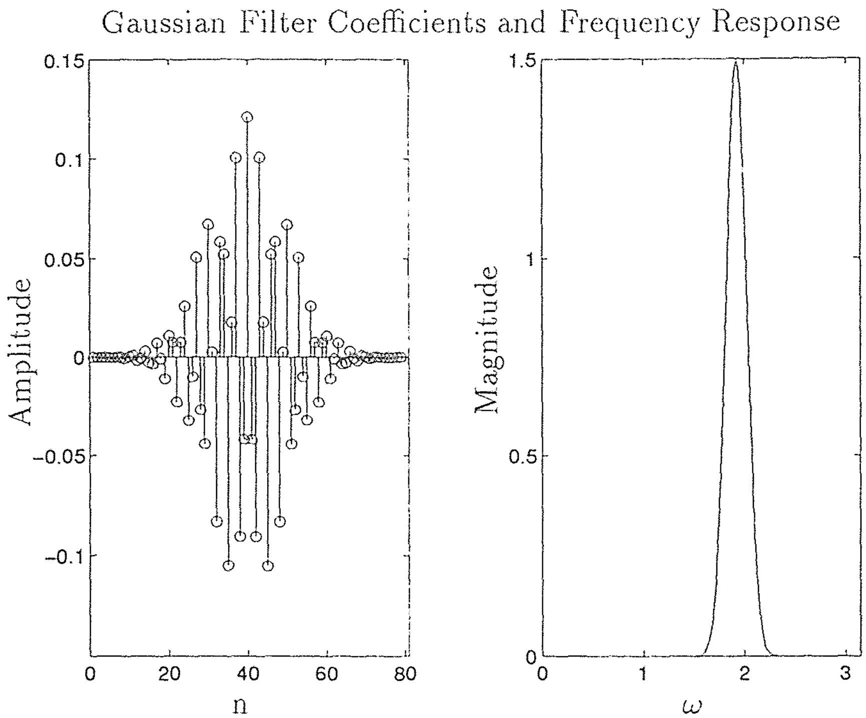

Figure 4.9 Gaussian Window Time and Frequency Response

window for the excision. In addition to that, a Binomial-Gaussian function will be an appropriate choice because of its smooth frequency response, and excellent frequency localization [6]. The general structure of a frequency window exciser is shown in Figure 4.8. By calculating the DFT of the received signal, the interference localizer examines the frequency localization of the interferences and their bandwidths. Using this data, the Gaussian window generator calculates the corresponding filter coefficients. The cosine modulator modulates the filter to the desired frequency (Figure 4.9). Filtering the signal with this linear phase FIR filter and subtracting from the received signal excises the interference. A comparator compares the excised signal with the excision margin and decides whether the excision goal is already achieved. If not, the operation is repeated. The Gaussian approximation of the Binomial coefficients [6] is used to estimate the Gaussian pulse, it can be written for $N \gg 1$,

$$\begin{pmatrix} N \\ k \end{pmatrix} \sim \frac{2^N}{\sqrt{N\frac{\pi}{2}}} e^{-\left\{\frac{(k-\frac{N}{2})^2}{\frac{N}{2}}\right\}}. \tag{4.11}$$

This Binomial sequence reassembles the Gaussian pulse successfully for large N. The factor of $(\frac{1}{2})^{N-1}$ normalizes the Binomial function's frequency response to one at $\omega = 0$. Therefore, for a practical implementation of the Binomial-Gaussian function,

$$f(k) = (\frac{1}{2})^{N-1} \begin{pmatrix} N \\ k \end{pmatrix} \tag{4.12}$$

can be used to replace the Gaussian pulse [6]

$$f(k) = \sigma\sqrt{\frac{A}{\pi}} e^{-\sigma^2 k^2} \tag{4.13}$$

$$|F(e^{j\omega})|^2 = Ae^{-\omega^2/2\sigma^2} \qquad |\omega| < \pi, \tag{4.14}$$

where the constant A is chosen so as to normalize the energy of the function to unity over $[-\pi, \pi]$. The bandwidth of the filter (σ) is determined by the variance of the Gaussian pulse. But the bandwidth in frequency is also related to the duration in time. Therefore, a closed-form relation is necessary between the duration (N) and bandwidth of the filter. This can be approximated by $N = \frac{4}{\sigma^2}$ as shown in [6]. For practical purposes, it is advised to restrict the length of the filter to maximum $N = 513$ taps. The modulation of the lowpass Gaussian window is performed using cosine modulation [2, 22]. The interference localizer estimates the center frequency ω_c of the interference. The window generator modulates the low-pass window $f(k)$ to the desired position according to [2],

$$f'(k) = f(k)\cos[\omega_c(k - \frac{N-1}{2})]. \tag{4.15}$$

One important point by using this modulated filters is power normalization. If the filters are normalized, the output can be directly subtracted form the delayed version of the input. This normalization causes $f(k)$ to be calculated as

$$f(k) = \frac{g(k)}{\sqrt{\frac{\pi E_g}{2\sigma}}} \tag{4.16}$$

where $g(k)$ is the Gaussian lowpass filter and E_g is its energy. E_g can be calculated as

$$E_g = \sum_{n=1}^{N} g(n)^2. \tag{4.17}$$

The Gaussian filter can be written as [7]

$$g(n) = \sigma\sqrt{\frac{K}{\pi}}e^{-(\sigma n)^2}. \tag{4.18}$$

The constant K can be calculated as follows

$$K = \frac{\sqrt{\frac{\pi}{2}}}{\sigma\, erf(\frac{\pi}{\sigma})}. \tag{4.19}$$

The normalization with $\frac{1}{\sqrt{\frac{\pi E_g}{2\sigma}}}$ is based on the unity magnitude response of a filter with bandwidth π. A filter with smaller bandwidth has to be normalized such that its energy is equal to $\frac{B}{\pi}$, where B is the Bandwidth of the filter. The simulation results for this exciser are presented in a later chapter.

4.3 Power Margin in Multitone Excisers

In the case of multitone excision one significant concern is the tradeoff in between further reduction of interferences and the decreasing desired signal power. This results in a bit error rate performance curve shown in Figure 4.10. This curve has a minimum point depending upon the number and power of the interferences, the noise power, and the loss of signal bandwidth due to the excision. Therefore, a threshold has to be found that takes this parameter into account. The received signal power can be written as

$$P_R = P_S + P_N + P_I + 2\sum_{k=1}^{N}\left[s(k)j(k) + s(k)n(k) + n(k)j(k)\right], \tag{4.20}$$

where P_S is the transmitted signal power, P_N the noise power, and P_I the interference power. The summation $\sum_{k=1}^{N}[s(k)j(k) + s(k)n(k) + n(k)j(k)]$ is zero, if the received signal components are orthogonal to each other. For practical applications, their correlation is small compared to the power of the signal components and therefore the sum. For this reason, we will neglect it. The first approximation of a parameter is an excision margin M_E which can be written as

$$M_E = P_S + P_N + M_0. \tag{4.21}$$

This margin takes into account that the excisers mainly reduce the narrow band interference power, but keep the wide spread signal and noise powers minimally affected. The constant M_0 is to ensure, that the iteration is stopped when the interferences are removed. The excision margin versus the SNR is plotted in Figure 4.11. This margin is proven to be useful for all simulations with narrow band interferences. For the excision of a much higher number of interferences as they occur in DAB, this margin is not optimal. This can be shown by observing the loss of bandwidth (see Fig. 4.12). For a small number of interferences, the undesired spectra are excised completely within a few iterations. Each interference will cause a gap in the spectrum. If the over all sum of excised bandwidths is small, the performance is good. The small amount of lost signal power forces the excised signal already underneath the fixed excision margin, while keeping the unaffected signal bandwidth large enough to ensure decoding. For a high number of interferences, the losses in bandwidths increases significantly. The remaining signal power can not produce enough processing gain to overcome the noise and therefore the system performance is poor. This can be seen in Figure 4.12, where an FM-interference is excised with different excision margin levels. Each iteration excises one interference. Starting from the most significant one, the excisers adapt their structure to the interferences and eliminate them. But on the same time the desired signal power decreases. This causes the system to be more affected by noise. An adaptive excision margin is needed to measure the tradeoffs between an additional excision operation and the accompanied decrease of SNR . This scenario can be mapped into a varying margin M_E. This margin starts from $M_E = P_S + P_N + M_0$ and increases in each iteration

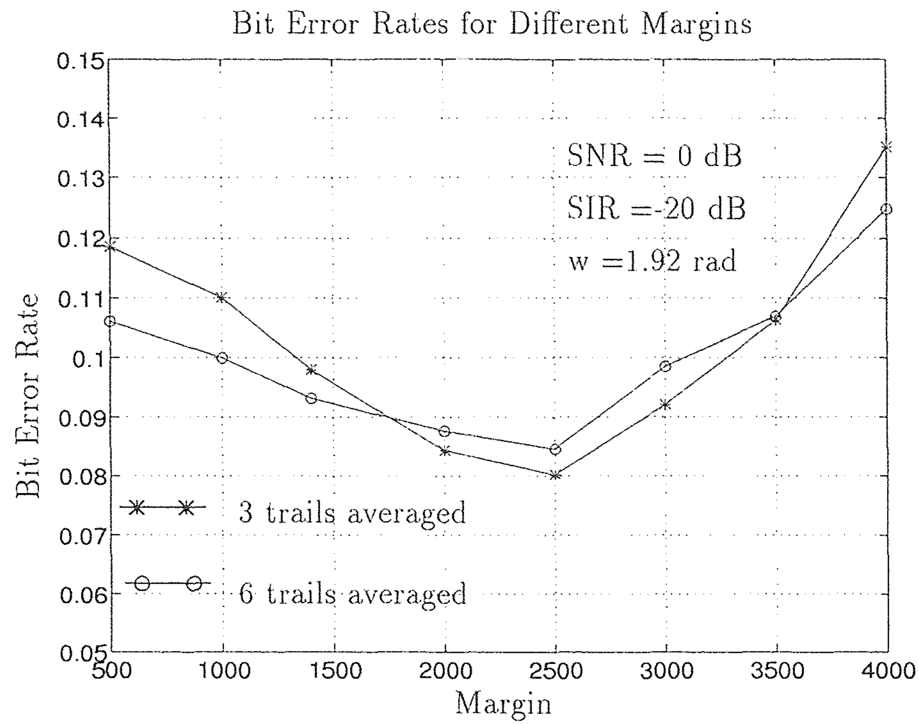

Figure 4.10 The Performance of a DSS System for Different Power Margins

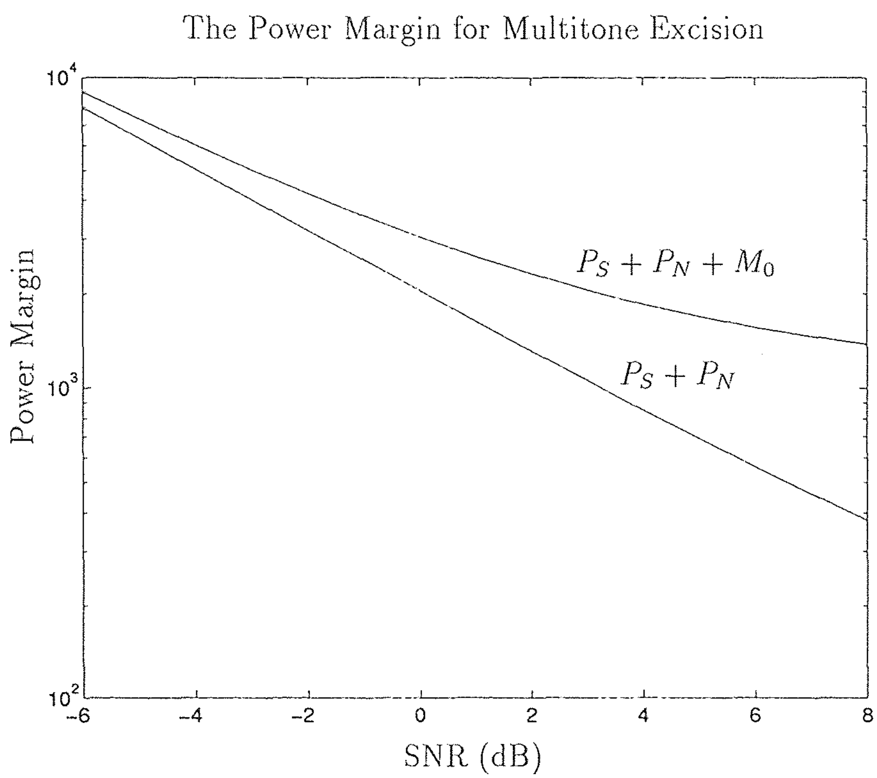

Figure 4.11 The Power Margin

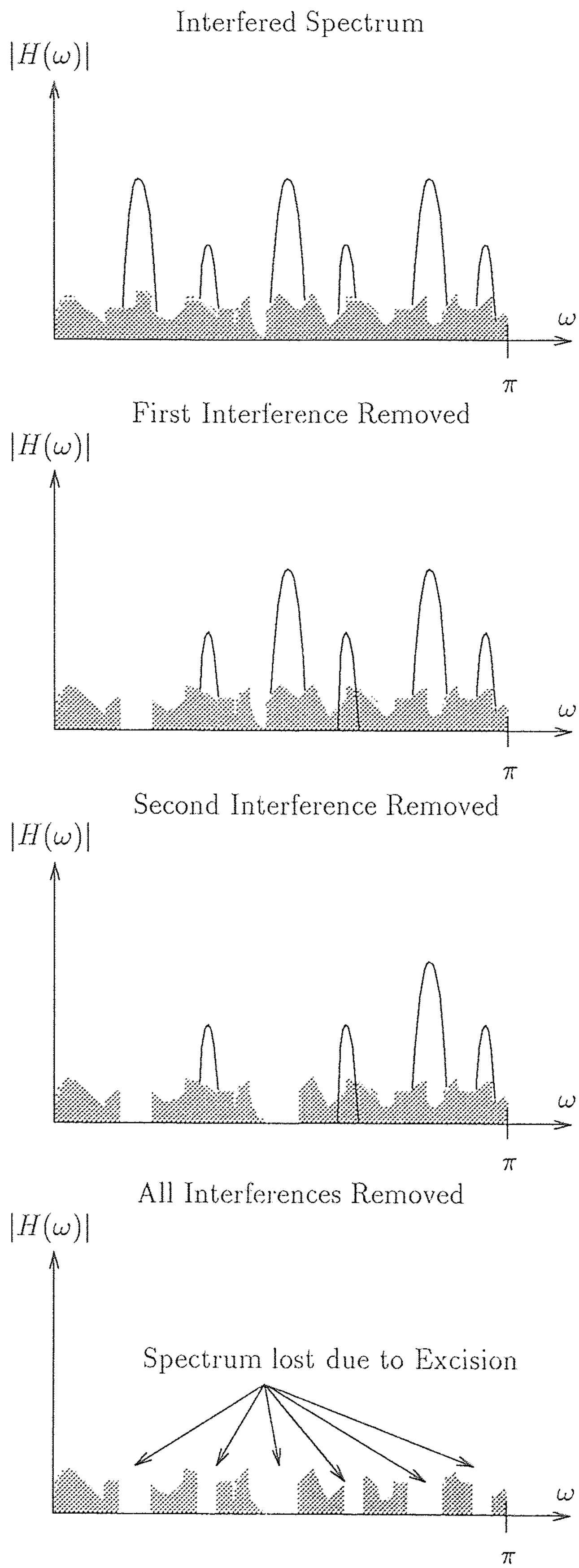

Figure 4.12 Spectral Losses Due to Excision

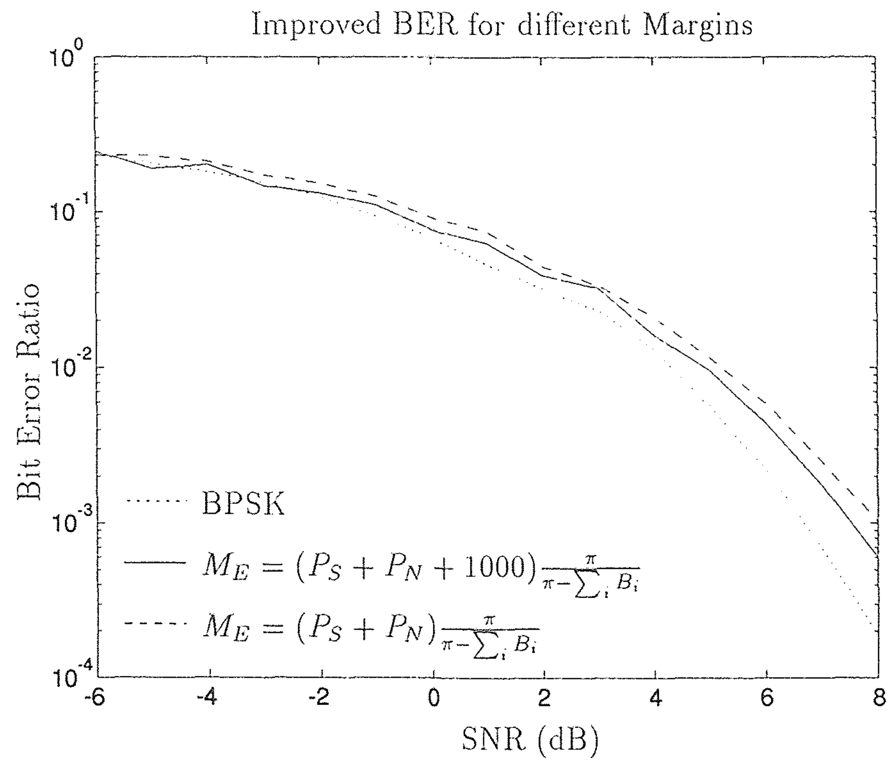

Figure 4.13 Improvement of Different Excision Margins

proportional to the lost bandwidth. The excision is performed until the overall signal power is less than this margin. This leads to the expression for M_E,

$$M_E = \frac{\pi}{\pi - \sum_{i=1}^{K} B_i} \left(P_S + P_N + M_0\right), \tag{4.22}$$

where B_i is the bandwidth of the i^{th} excision-filter and K the number of interferences excised. This excision margin model is based on the assumption, that the spreaded signal power is linearly distributed within $[0, \pi]$. In addition we assume that a loss of B_k bandwidth will cause a decrease in spreading gain of $\frac{\pi}{B_K}\%$. The performance for different adaptive excision margins are shown in Figure 4.13 for single tone interferences.

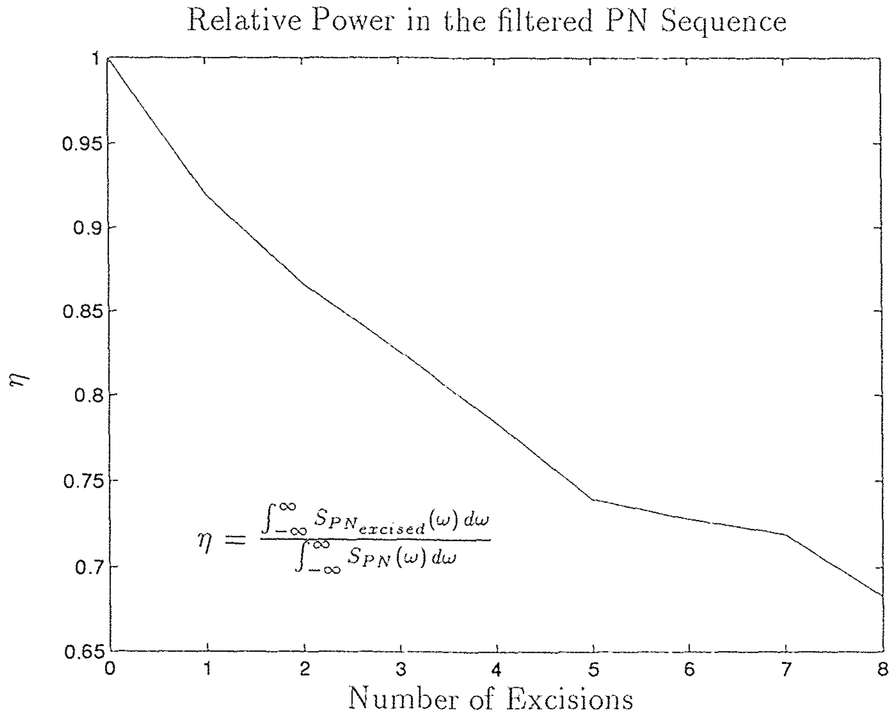

Figure 4.14 Power Loss Due to Excision

4.4 Impact of Multiple Filtering Operations on PN-Sequences

An important issue for multitone excision is the impact of the required filtering operations on the PN-sequence. The equalization of the filtered signal would recover the interference. Therefore, the filtered PN-sequence has to be studied to ensure that the excision operation did not destroy their properties. Since the exact number of interferences and their spectral localization is unknown in DAB, we took one example set of filters used to excise a multitone interference. This set of filters (Figure 4.17) is used to estimate the changes on the PN-sequence. The correlation receiver used for despreading depends mainly on the time function of the signal and their changes. Therefore, we filtered the PN-sequence consecutively with these 8 filters and plotted the time functions of the PN-sequences. Figure 4.15 shows the original PN-sequence and its distorted versions due to the excision operations. These changes are caused by the loss of spectral components in the vicinity of the excised interferences. To visualize this, the DFT of the PN-sequence and its excised version is plotted in

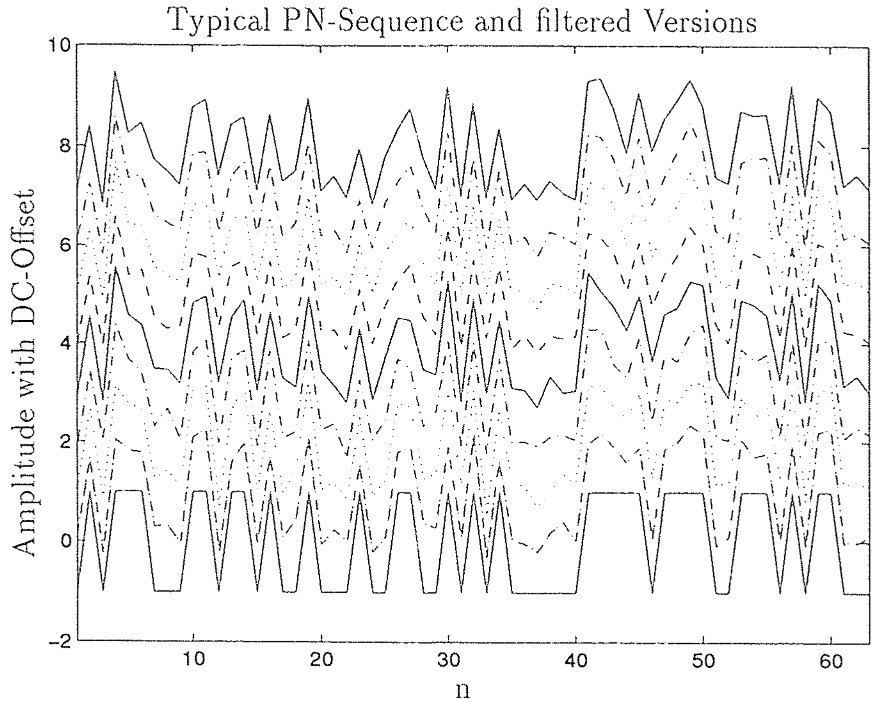

Figure 4.15 Time Functions of a Typical PN-Sequence and Filtered Versions

Figure 4.16. The decision variable of the receiver is mainly depending on the power of the PN-sequence and its correlation with the original version. Figure 4.14 shows the relative loss in power of the PN-sequence. Analyzing all this we can say that the filters do not cause a significant decay of the pn-sequence properties in this example.

4.5 Signal to Noise and Interference Ratio Improvement

One important observation for excisers is the signal to noise improvement. This parameter gives an insight into the gain of the excision operation. The SNIR used here is defined at the output of the exciser (Fig. A.7). The SNIR can be written as

$$SNIR = 10\ \log_{10} \frac{P_S}{P_{NI}}, \tag{4.23}$$

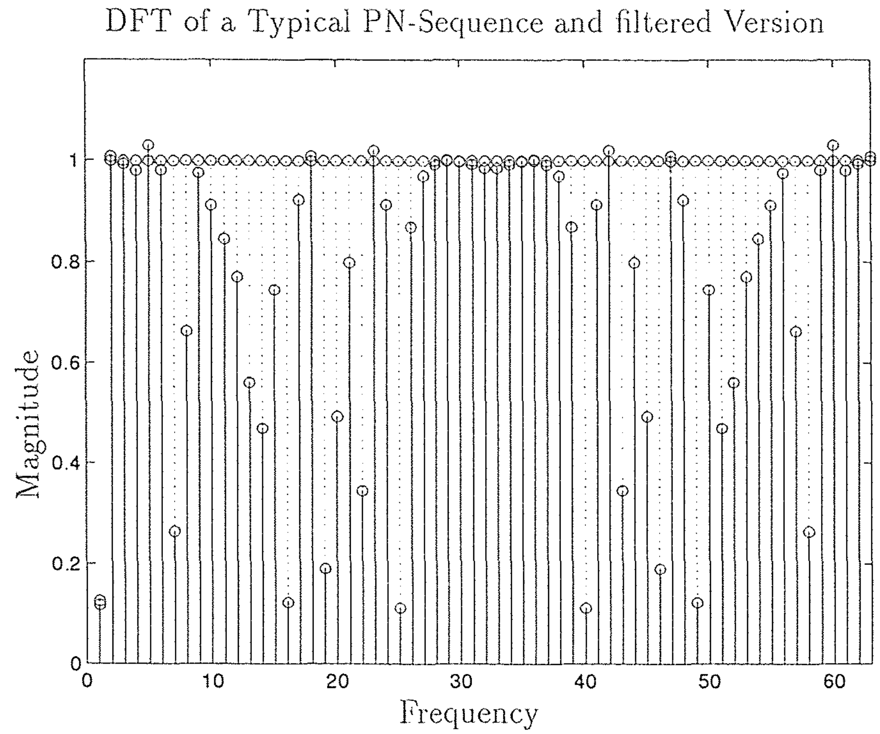

Figure 4.16 Filtered Spectrum of a PN-Sequence

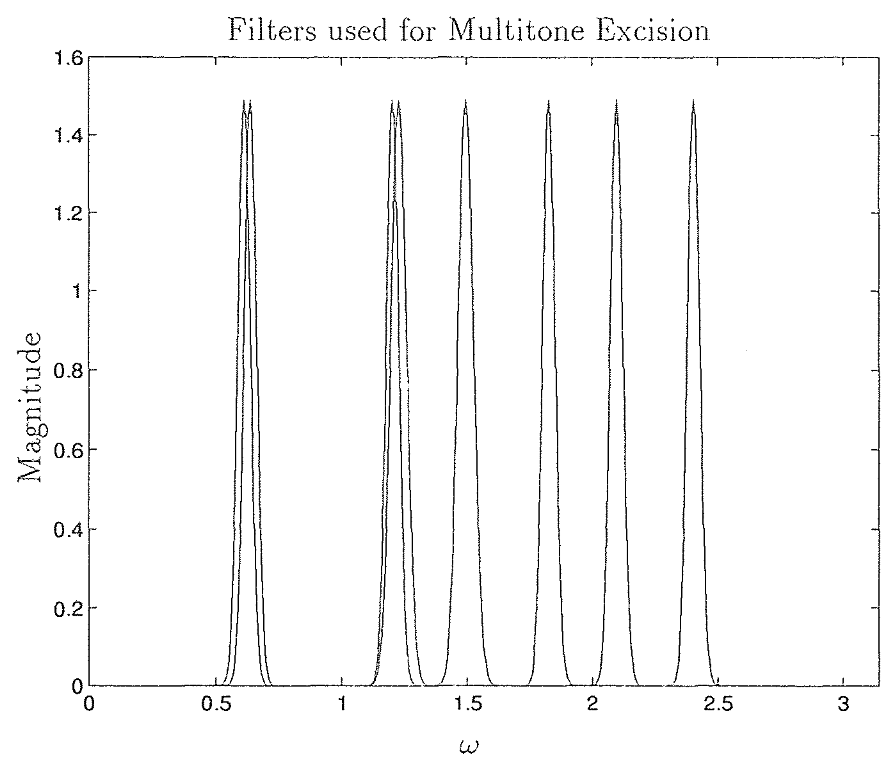

Figure 4.17 Gaussian Filters Used for Multitone Excision

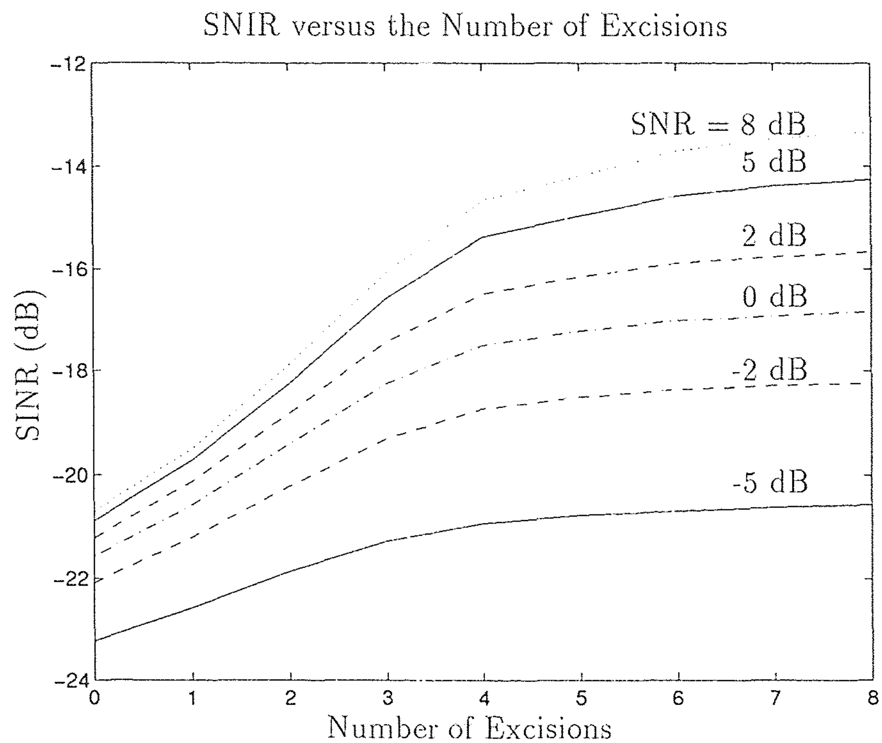

Figure 4.18 SNIR for an FM Signal Versus the Number of Excisions

where the signal power is P_S, the noise and interference power is P_{NI} respectively. The power of the signals are calculated as follows

$$P_x = \sum_{i=1}^{N} x^2(i) \tag{4.24}$$

where N is the length of one databit and x the data or noise signal. Since the normal received signal is the combination of signal noise and interference, the data-signal was processed independent from the received signal, using the same filters. This filtered version of the data-signal is subtracted from the excised version of the received signal, such that two separate signals are obtained. The interference/noise signal and the data signal respectively. This two signals are squared and summed over one bit duration and the power ratio is calculated. The power ratios $\frac{P_S}{P_{NI}}$ are averaged over 3 symbols before the SNIR is calculated. The simulation system for the evaluation is shown in Figure A.7 and the table of parameters used for this simulation are given in Table A.3.

Figure 4.18 shows the performance of the Gaussian window based exciser for FM-interference versus the number of excisions. The simulation was repeated for different noise levels, to visualize the affects of noise within the system. It can be seen, that after 6-7 excisions the SNIR reaches a limit. This can be interpreted as that the significant components are excised. From this point on the decrease in interference is accompanied by a decrease of the energy of the PN-sequence.

CHAPTER 5

The DAB Transmission

5.1 The Requirements for In-Band On-Channel Transmission

The In-Band On-Channel transmission of the new DAB-service is restricted by several practical considerations. Some of them are stated below to explain the restrictions to meet in a design of a DAB-System [14].

5.1.1 FM Requirements

For the FM In-Band On-Channel transmission the following specifications are given:

⇒ the DAB-signal must be In-Band On-Channel, and not create perceptible disruption to the analog FM signal

⇒ the DAB signal must fit within the existing FM bandwidth of $200kHz$

⇒ the DAB signal must be 30dB below the analog FM signal

⇒ the supportable data rate must be an aggregate $400kbits/sec$

⇒ the modulation format must be able to withstand multipath fading with the following characteristics:

- $100kHz$ wide and $15dB$ deep for stationary reception
- $200kHz$ wide and $20dB$ deep for mobile reception

5.1.2 AM Requirements

For the AM In-Band On-Channel transmission the following specifications are given:

⇒ the DAB-signal must be In-Band On-Channel, and not create perceptible disruption to the analog AM signal

⇒ the DAB signal must fit within the existing FM bandwidth of $20kHz$

⇒ the DAB signal must be 35dB (co-channel) and 25dB (adjacent channel) below the analog AM signal

⇒ the supportable data rate must be an aggregate in the range of $96-128kbits/sec$

⇒ the modulation format must be able to withstand multipath fading with the following characteristics:

- $100kHz$ wide and $15dB$ deep for stationary reception
- $200kHz$ wide and $20dB$ deep for mobile reception

5.2 DAB on FM

As we have seen in chapter 3, the FM-reception does not put any requirements on the amplitude of the incoming signal. Furthermore, the practical receiver handles amplitude related errors by slicing the incoming signal around zero. Using the remaining zero crossings, the FM-signal is recovered with normalized amplitude. A transmission scheme for this property will be discussed in the first part of this chapter. The second part proposes a way of reducing the interfering affects of the analog FM-signal to the digital separately transmitted signal for the case of DSSS-DAB.

5.2.1 AM Modulation on FM

The first technique of transmitting digital audio on an FM-signal is to use a conventional amplitude modulation. This technique makes use of the amplitude normalization of FM-receivers. The data recovery can be easily managed using envelope detection. A simple block diagram of such a receiver is shown in Figure 5.1. In this transmission system the analog audio signal is FM-modulated using the conventional techniques. This FM-signal is then AM-modulated with the digital DAB-signal.

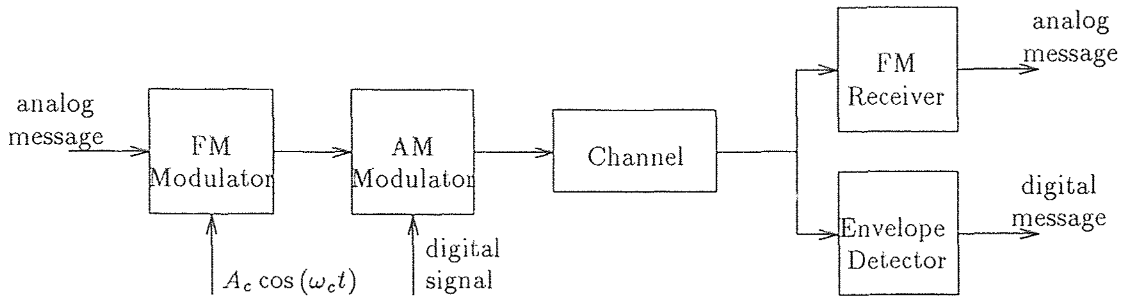

Figure 5.1 FM DAB Transmission System Block Diagram

This composite signal is displayed in Figure 5.2. The FM-receiver can easily recover the analog audio information by evaluating the zero crossings for demodulation. The DAB-receiver will perform an envelope detection on the FM-DAB-signal. The detector is unaffected by the FM-frequency changes, since these deviations are negligible compared to the carrier frequency.

To evaluate the performance of the AM-modulated FM-DAB-System, a simulation system was developed using Comdisco's SPW. The detailed simulation parameter and simulation blocks are shown in the Appendix in Table A.1 and Figure A.1.

5.2.1.1 Simulation of the System Transmitter

The transmitter for the DAB-transmission as an AM-modulated FM-signal is shown in Figure A.2. The binary, bipolar, white data sequence $d(t)$ is pulse shaped using a raised cosine filter. The constant multiplier K_a is used to adjust the DAB-signal power and AM modulation amplitude sensitivity k_a. After adding the signal to one, the DAB-signal is

$$s_{DAB}(t) = (1 + K_a p(t)) \tag{5.1}$$

where

$$p(t) = \int_{-\infty}^{+\infty} d(\tau)h(t-\tau)\,d\tau, \tag{5.2}$$

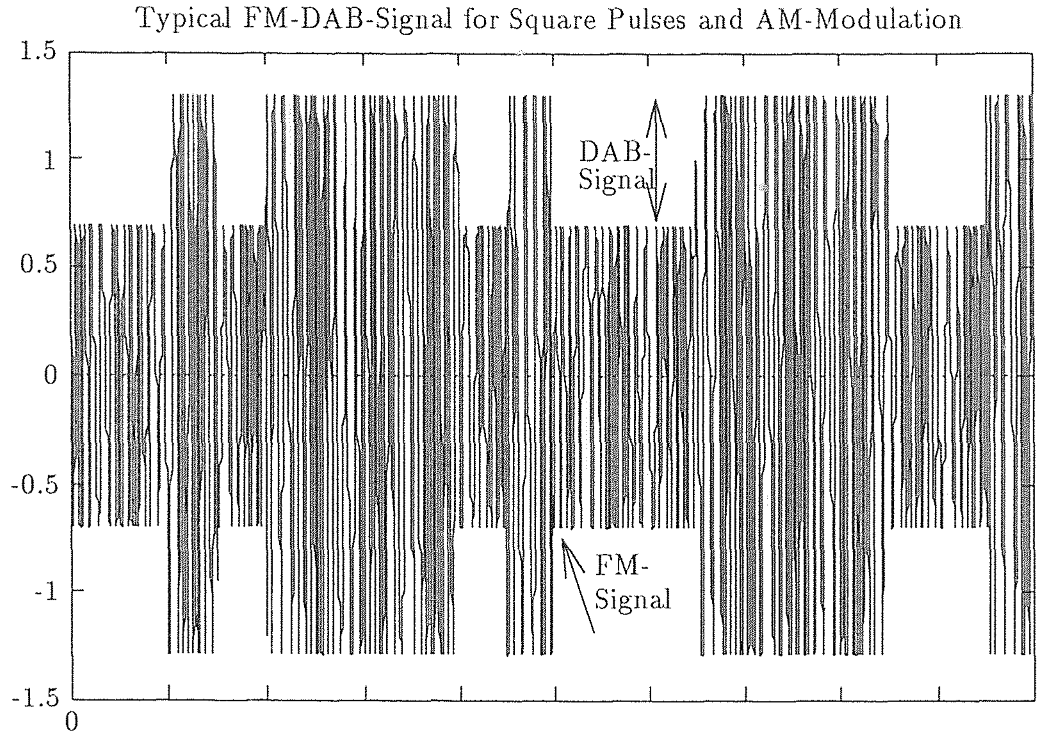

Figure 5.2 FM DAB Signal for AM-Modulated DAB

where $h(t)$ is a raised cosine pulse,

$$h(t) = \left[\frac{\sin\left(\frac{\pi t}{T}\right)}{\frac{\pi t}{T}}\right]\left[\frac{\cos\left(\frac{\alpha\pi t}{T}\right)}{1-\left(\frac{2\alpha t}{T}\right)^2}\right]. \tag{5.3}$$

SPW requires the use of sampled signals, therefore replacing t by nT_s

$$s_{DAB}(nT_s) = (1 + K_a T_s \sum_{l=-\infty}^{+\infty} d(l)h(nT_s - l)), \tag{5.4}$$

where $f_s = \frac{1}{T_s}$ is the sampling frequency. The FM-signal is generated and multiplied by a constant K_f, for normalized FM-power. This signal can be written as

$$s_{FM}(t) = K_f A_c \cos\left(2\pi f_c t + 2\pi k_f \int_0^t m(t)\,dt\right). \tag{5.5}$$

This is equivalent to simulating the sampled version,

$$s_{FM}(nT_s) = K_f A_c \cos\left(2\pi f_c nT_s + 2\pi k_f T_s \sum_{k=0}^{nT_s} m(k)\right). \tag{5.6}$$

These two signals are multiplied such that the transmitted signal $s(t)$ or $s(nT_S)$ is

$$s(t) = s_{FM}(t)s_{DAB}(t) = (1 + K_a\, p(t))K_f A_c \cos\left(2\pi f_c t + 2\pi k_f \int_0^t m(t)\, dt\right), \quad (5.7)$$

$$s(nT_s) = (1 + K_a\, p(nT_s))K_f A_c \cos\left(2\pi f_c nT_s + 2\pi k_f T_s \sum_{k=0}^{nT_s} m(k)\right). \quad (5.8)$$

This signal is transmitted using a flat, additive white Gaussian noise channel.

5.2.1.2 Simulation of the Receiver

The receiver, shown in Figure A.3 splits the signal into two paths. The upper path recovers the analog FM-audio signal while the DAB-signal is recovered in the lower path. The received signal can be written as

$$r(t) = A_r(t) \cos\theta_r(t), \quad (5.9)$$

where the amplitude of the signal is

$$A_r(t) = (1 + K_a\, p(t))K_f A_c, \quad (5.10)$$

and the angle of the carrier,

$$\theta_r(t) = \left(2\pi f_c t + 2\pi k_f \int_0^t m(t)\, dt\right). \quad (5.11)$$

Using $r(t)$ as the input to the hard limiter, the output signal can be written as a Fourier series [10]

$$v(t) = \frac{4}{\pi}\left[cos\theta_r(t) - \frac{1}{3}cos3\theta_r(t) + \frac{1}{5}cos5\theta_r(t) - ...\right]. \quad (5.12)$$

This signal is filtered with a Butterworth bandpass filter to recover the sinusoidal waveform, that can be written assuming optimal filtering as

$$e(t) = \frac{4}{\pi}cos\theta_r(t). \quad (5.13)$$

The PLL locks onto this signal to demodulate the analog FM. The output of the PLL is lowpass filtered and can be written as

$$e_{FM}(t) \approx \frac{4}{\pi}\frac{k_f}{k_v}m(t) \quad (5.14)$$

The DAB path of the receiver first recovers the envelope of the FM-signal. This signal can be written as,

$$v_{DAB}(t) = (1 + K_a p(t)) k_f A_c \tag{5.15}$$

To recover the bipolar digital data, it is necessary to subtract the mean, which is done using a comb filter. This filter estimates the mean of the signal by averaging it over a sliding time window. This mean estimate is then subtracted form the signal. The comb-filter has a transfer function $H\left(e^{-j\omega}\right)$ as follows,

$$H\left(e^{-j\omega}\right) = 1 - \frac{1}{N} \frac{\sin\left(\omega \frac{N}{2}\right)}{\sin\left(\frac{\omega}{2}\right)} e^{-j\omega \frac{N-1}{2}}, \tag{5.16}$$

where N is the length of the sliding window. The output of the filter is

$$e_{DAB}(t) = \int_{-\infty}^{\infty} v_{DAB}(t-\tau) h(t)\, dt \approx K_a p(t) k_f A_c, \tag{5.17}$$

a scaled version of the input signal. To reduce the amplitude distortion, the filtered signal is sampled and sliced around zero, to recover the digital data.

5.2.2 DSSS DAB in FM

The second technique of transmitting DAB digital data In-Band On-Channel is to use a spread spectrum signal underneath the analog FM. This transmission scheme makes use of the interference resistance of a spread spectrum system. To evaluate the performance of the DSSS under an analog FM-signal, a simulation system was developed using SPW. The main components of the system are shown in Figure A.5. This system consists of a spread spectrum data source, a channel that adds the interferences and noise, an exciser and a receiver for spreaded data. The additional blocks take care of the bit error rate evaluation.

5.2.2.1 Simulation System for FM-DAB + Gaussian Noise Channel

The Data Generator is shown in detail in Figure A.2. It generates a white binary data signal. This signal is converted into a bipolar signal and multiplied bit by bit with the bipolar PN-sequence. Hereby, the sampling frequencies are chosen, such that one data bit is replaced by the pn-sequence. This spreaded signal is degraded by additive white Gaussian noise. In addition to that an FM-signal is added to the spreaded data. This SPW-block is shown in Figure A.6. The received signal can be written as

$$\underline{r}_l = d_l\underline{c} + \underline{n}_l + \underline{s}_{FM}, \tag{5.18}$$

where $\underline{s}_{FM}$ is a vector of FM signal samples according to

$$s_{FM}(n) = A_c \cos\left(2\pi f_c n + 2\pi k_f \sum_{k=0}^{n} m(k)\right). \tag{5.19}$$

Before decoding the digital data, the excision block has to reduce the interferences. Therefore, a Binomial-Gaussian Window based exciser adapts a filter structure to the spectral needs of the FM-signal and excises the main components of the FM signal. The adaptive excision power margin is chosen according to Eq. (4.22). The constant M_0 is equal to 1000 for our simulations.

The output of the exciser for the m^{th}-data bit can be written as

$$y(n) = \sum_{k=-\infty}^{\infty} r(k)h(n-k), \tag{5.20}$$

$$\begin{aligned} y(n) = \quad & \sum_{k=-\infty}^{\infty} d_m c(k)h(n-k) \\ + \quad & \sum_{k=-\infty}^{\infty} j(k)h(n-k) \\ + \quad & \sum_{k=-\infty}^{\infty} n(k)h(n-k), \end{aligned} \tag{5.21}$$

where $h(k)$ is the combined version of all used excision filters.

The Despreading is done using the same proper synchronized PS sequence as used at the transmitter. The decoder block is shown in Figure A.11. After multiplication with the PN sequence the decoder sums the samples of one data bit and decides by evaluating the sign of the signal. The output of the summation operation can be written as

$$d'_m = \sum_{n=1}^{N} y(n)c(n) \tag{5.22}$$

$$\begin{aligned} d'_m = \quad & \sum_{n=1}^{N} c(n) \sum_{k=-\infty}^{\infty} d_m c(k)h(n-k) \\ + \quad & \sum_{n=1}^{N} c(n) \sum_{k=-\infty}^{\infty} j(k)h(n-k) \\ + \quad & \sum_{n=1}^{N} c(n) \sum_{k=-\infty}^{\infty} n(k)h(n-k), \end{aligned} \tag{5.23}$$

where N is the length of the PN sequence and $c(n)$ the PN sequence. The decision is based on the sign of d'_m. The decoded data bit is then compared with the original transmitted version. The error counter compares both signals and registers every bit error occurring. If the desired number of bit errors occurred, the simulation is stopped and the output file can be used for bit error calculation.

5.3 DAB on AM

Since the normal AM-receiver is using non-coherent demodulation techniques, one way of transmitting digital data over an AM-channel is to use the phase of the carrier. In this case, a receiver for the standard analog AM is unaffected, but a coherent DAB receiver will easily demodulate the digital data. This system configuration is shown in Figure 5.3. The received signal can be written as

$$r_{DAB}(t) = A_c[1 + k_a m(t)]cos(2\pi f_c t + \theta_d(t)) + n(t). \tag{5.24}$$

$\theta_d(t)$ in Eq. (5.24) represents the M-PSK-modulation. The reception is done in two separated paths. The upper one recovers the analog data using any noncoherent demodulation technique. Therefore, the output of the envelope detector is

$$y(t) \simeq A_c[1 + k_a m(t)] + n_c(t). \tag{5.25}$$

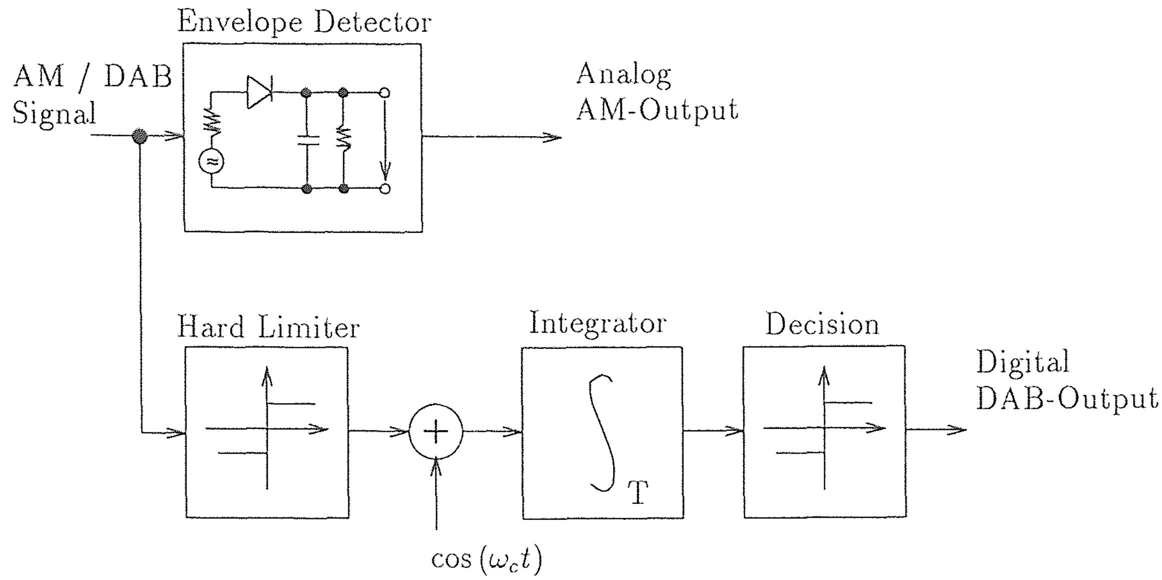

Figure 5.3 DAB System (AM)

The digital data is recovered using coherent demodulation. The output of the hard limiter can be written as a Fourier series [10]

$$v(t) = \frac{4}{\pi}\left[cos\theta_r(t) - \frac{1}{3}cos3\theta_r(t) + \frac{1}{5}cos5\theta_r(t) - ...\right], \tag{5.26}$$

where

$$\theta_r(t) = 2\pi f_c t + \theta_d(t) + \theta_n(t). \tag{5.27}$$

Here $\theta_n(t)$ is the phase-error caused by the noise of the channel. The demodulation with a proper synchronized Cosine generator moves the signal into baseband. The integration over a bit-duration recovers the digital data. The high frequency components will integrate to zero, since the bitlength should be chosen to be a integer multiple of the carrier period. Therefore the decision variable λ_k for the k^{th}-bit is given by

$$\lambda_k = \frac{1}{T_d}\int_{(k-1)T_d}^{kT_d} \cos(2\pi f_c t) v(t)\, dt. \tag{5.28}$$

CHAPTER 6

RESULTS

In this chapter the results for different simulations are given.

6.1 The Excision of Multitone Sinusoidal Interferences

To estimate the performance of the Binomial-Gaussian Window-based exciser, different numbers of sinusoidal interferences were used to disturb the signal. The performance of the Exciser was evaluated for different number of bits used for the excision. The parameters of the interference are given in Table 6.1. The over all signal to interference ratio was held constant at $SIR = -20dB$ The Bit error rate

Parameter	Frequency	Amplitude
One Interference	0.1885 rad/sec	14.14
Two Interferences	0.1885 rad/sec	10.00
	0.3770 rad/sec	10.00
Three Interferences	0.1885 rad/sec	7.071
	0.3770 rad/sec	10.00
	0.5655 rad/sec	7.071
Four Interferences	0.1885 rad/sec	7.071
	0.3770 rad/sec	7.071
	0.5655 rad/sec	7.071
	1.0681 rad/sec	7.071

Table 6.1 The Simulation Parameters for the Multitone Interference Excision

for different signal to noise ratios is shown in Figure 6.1. To improve the performance for more than one interference the bit error rate was evaluated for blocks of more than one bit. Thereby, the performance was improved by increasing blocksize. A plot of the bit error rate for 3 bit blocksize is given in Figure 6.2.

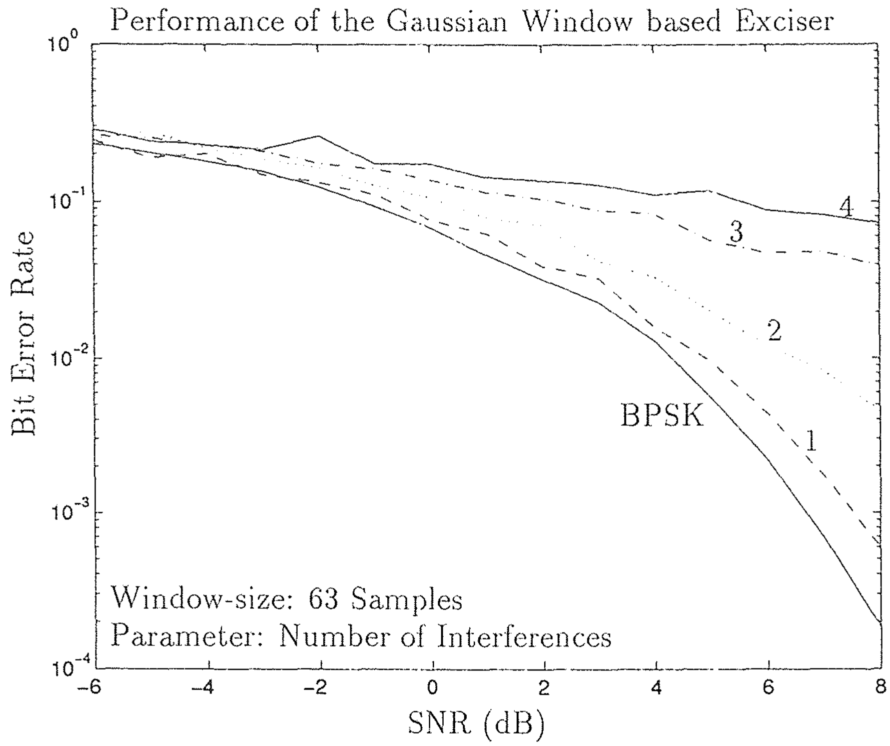

Figure 6.1 Performance of Gaussian Window-Based Exciser for a 63 Samples Window

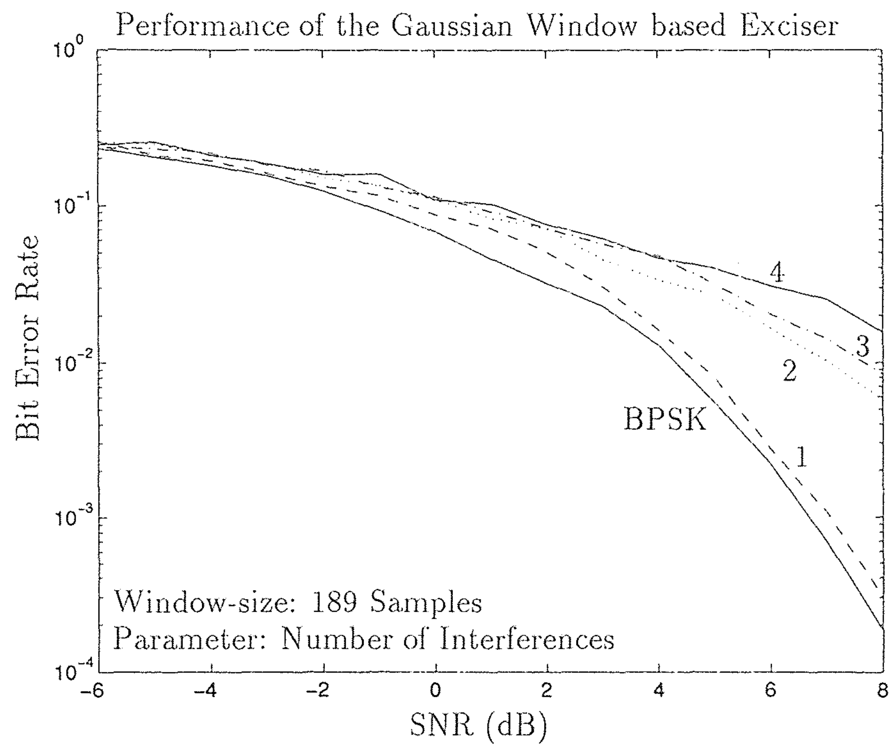

Figure 6.2 Performance of Gaussian Window-Based Exciser for a 189 Samples Window

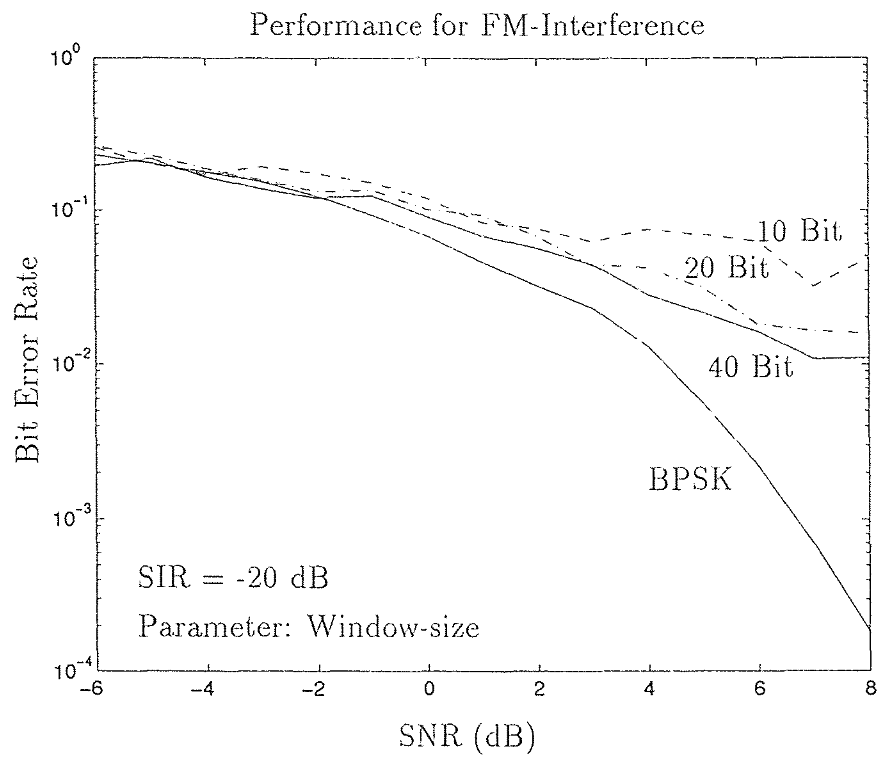

Figure 6.3 Performance of Gaussian Window-Based Exciser for FM-Interference

6.2 FM Interference Performance

The simulations for FM interference were done using the system shown in Figure A.4. The interfering FM is generated using a slowly changing modulation frequency with random phase $\{-\pi, \pi\}$. The bandwidth of the interference is chosen such that the PN-sequence and the interference occupies the same bandwidth. Excision is done using the modulated Gaussian Window exciser with an adaptive excision margin, as shown before. The performance was evaluated for different window sizes. This window size is the number of data bits, used for the excision operation. Each data bit is sampled 63 times. The increase of performance is due to the better frequency localization of the interference in case of longer windows. The exciser examines first the Fourier transform of the received signal. Using this spectral representation the localization and bandwidth of the interferences are evaluated. With more detailed

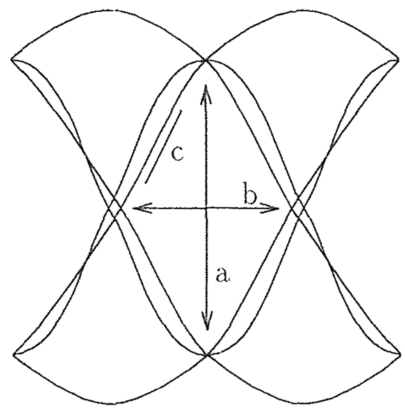

a) indicates immunity to noise
b) indicates the immunity to timing phase
c) indicates sensitivity to jitter in timing phase

Figure 6.4 Estimation of System Performances using the Eye Diagram [11]

Fourier transform coefficients, more bits are used, the spectral representation better. Therefore, the bandwidth and localization of the interferences are measured more precise. This allows the generation of narrow windows, that keep the loss of spectrum small.

6.3 Performance of AM-Modulated FM

The performance of the AM modulated DAB can be seen in Figure 6.5, where an eye-diagram of the received pulse is shown. The eye diagram allows the estimation of transmission parameters. Figure 6.4 shows the parameters, that can be estimated using the eye-diagram. Comparing this with the simulated diagram shows, that noise is no problem in this transmission. In addition to that, the system is robust against timing jitter.

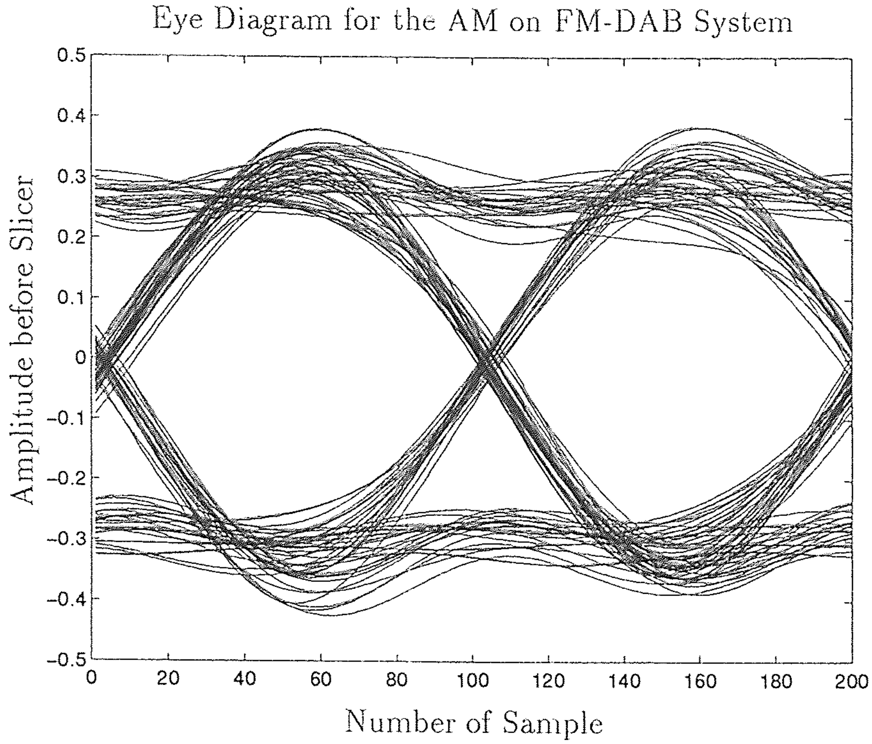

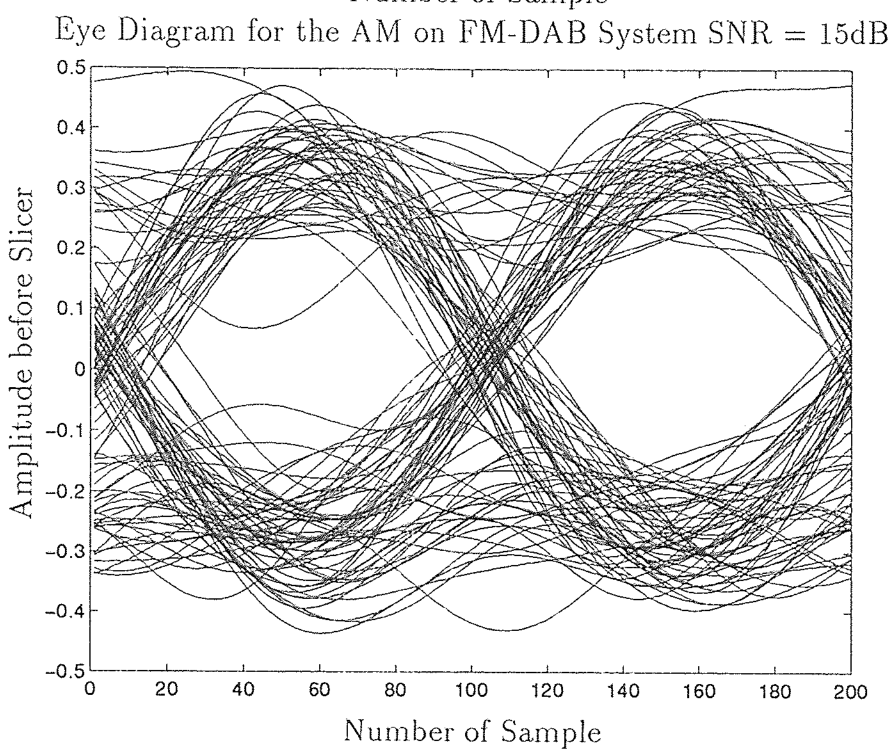

Figure 6.5 Eye Diagrams of the AM on FM-DAB System

CHAPTER 7

DISCUSSION AND CONCLUSIONS

In this thesis, we exploit the in-band on-channel transmission of digital audio data for DAB applications. Several different transmission scenarios were employed and simulated. In this chapter, we will summarize the work we have done and discuss the results we established as well as the yet open questions, that have to be exploited in future work.

The main focus of this work was the usage of excision techniques for the direct sequence spread spectrum transmission of digital data and the exploration of the problems and solutions for this kind of transmission. The transmission of digital data underneath an FM signal using direct sequence spread spectrum transmission techniques requires the reduction of the FM interference using excision techniques. We developed and tested several excision algorithms and simulated their performance. The Binomial-Gaussian window-based exciser was used for FM excision because of its simplicity and implementability as well as its good performance. It requires no previous knowledge of the received signal or its statistics. The excision goal, the reduction or elimination of interfering signals, can be specified using an excision power margin that measures the energy of the remaining signal. If the excised signal energy is below this threshold the excision is stopped and the signal is decoded. The excision of interferences in DSSS performs very well for single or several tone interferences. In the FM interference case, the excision of main interferences is not sufficient to establish an acceptable bit error rate. The reason is that the repeated excision of interferences reduces the unaffected bandwidth. In addition to that, the unexcised bandwidth is not interference free, in contrast to the single tone case. The small but existing amount of interfering power, in addition to the lost bandwidth, decays the receiver performance. The system performance can be improved by extending the length of the window used for excision to several bits. However, the bit error rate results still do not allow a stable transmission of digital data underneath an FM signal.

The second approach to establish a digital transmission of audio data in-band on-channel, exploit in this thesis, is the usage of a AM modulation on the FM-signal. This approach holds a stable data transmission with a low bit error rate. In addition, the interference between the new service and the analog transmission is negligible. In contrast to the first approach, the digital data is unaffected by the analog transmission and therefore no excision has to be performed.

The third transmission scheme is used for the AM-DAB. There, the phase modulation of the carrier adds the new service to the analog signal. This transmission scenario allows the two signals to be detected independently from one another. Therefore, an interference reduction in the digital transmission, as well as in the analog transmission, is not necessary. The bit error rate of the AM-DAB transmission is only due to channel noise. Therefore it is capable of transmitting digital audio data in-band on-channel.

7.1 Future Work

This thesis examined the digital audio transmission in-band on-channel for DAB applications in the United States. Future research is necessary to fully exploit the practical merits of the transmission techniques mentioned above. More realistic channel scenarios have to be developed and examined. Attention has to be paid to issues such as channel fading and multipath reception. These practical problems of radio transmission in a mobile environment will require the use of more sophisticated receiver structures e.g. equalizers. In addition, the synchronization of these receivers to changing channel parameters and signal phases has to be exploited. Moreover analytical research has to be done to find optimal parameters for these problems. Finally, the implementation of the best solution in hardware and measurements in real environments will complete this work.

APPENDIX A

SIMULATION SYSTEMS

Parameter	Value
FM / DAB - Signal Source	
Data Bitrate	10 Bits/sec
Data Sampling Frequency	1000 Hz
Raised Cosine Filter (Order)	64 Taps
Roll-Off Factor	0.8
Frequency Deviation	6 Hz/V
Carrier Frequency	100 Hz
Sampling Frequency	1000 Hz
Audio Frequency	1 Hz
Audio Sampling Frequency	1000 Hz
Receiver	
PLL - Center Frequency	100 Hz
PLL Loop Filter (Order)	1
PLL Loop Filter (Bandwidth)	10 Hz
PLL VCO Constant	12
PLL Sampling Frequency	1000 Hz
Mean Estimator (Window)	10000 Samples
DAB - LP (Order)	20
DAB - LP (Passband)	12 Hz
DAB - LP (Sampling Frequency)	1000 Hz

Table A.1 The Simulation Parameters for the AM on FM DAB System

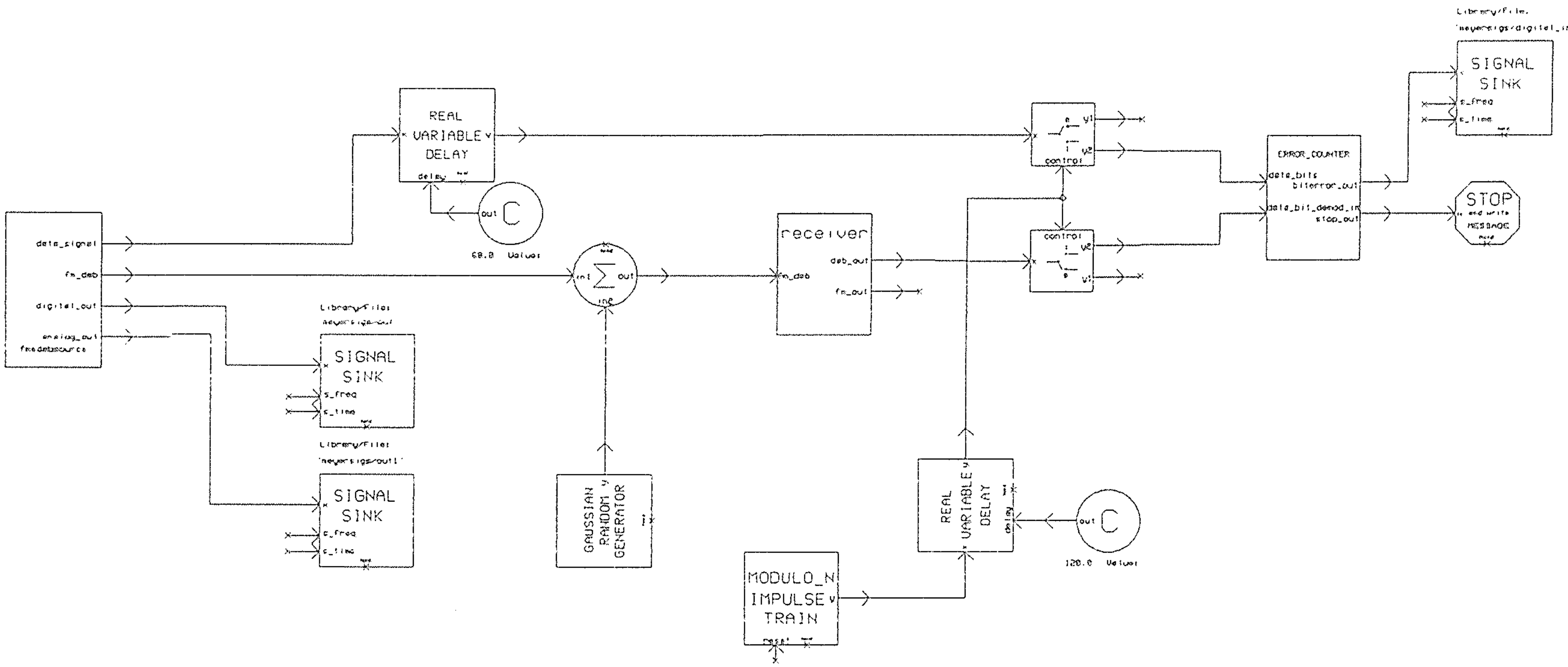

Figure A.1 The Simulation System for the AM on FM DAB System

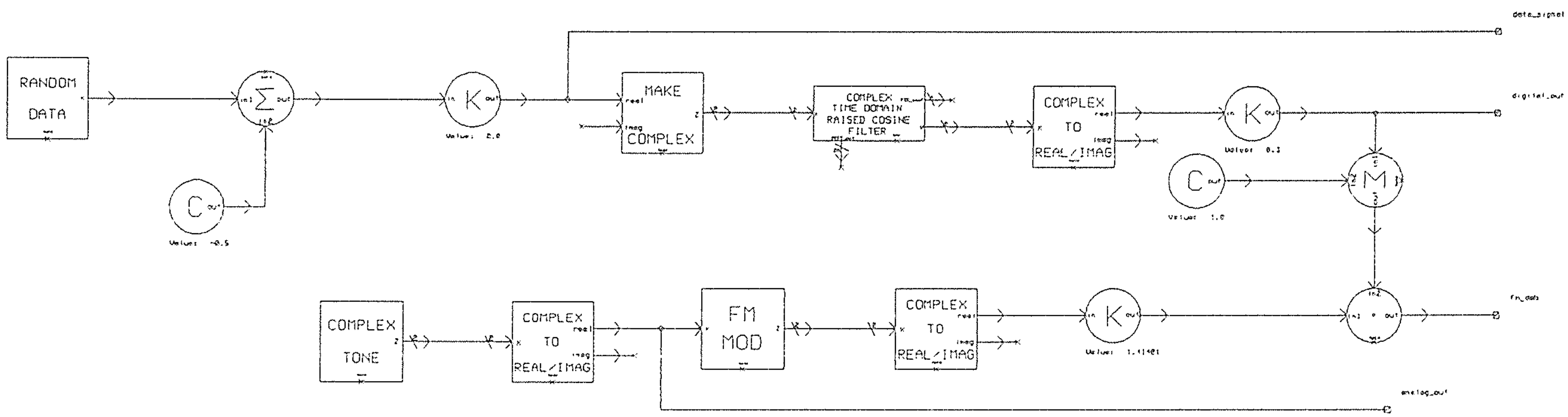

Figure A.2 Detail of the Transmitter for the AM on FM DAB System

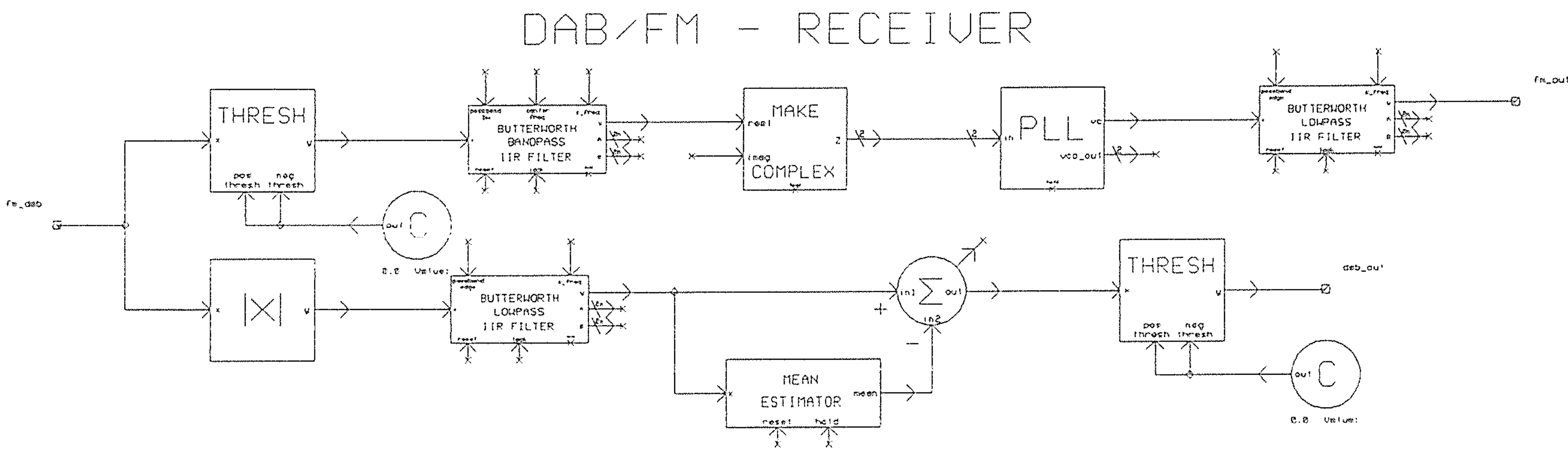

Figure A.3 Detail of the Receiver for the AM on FM DAB System

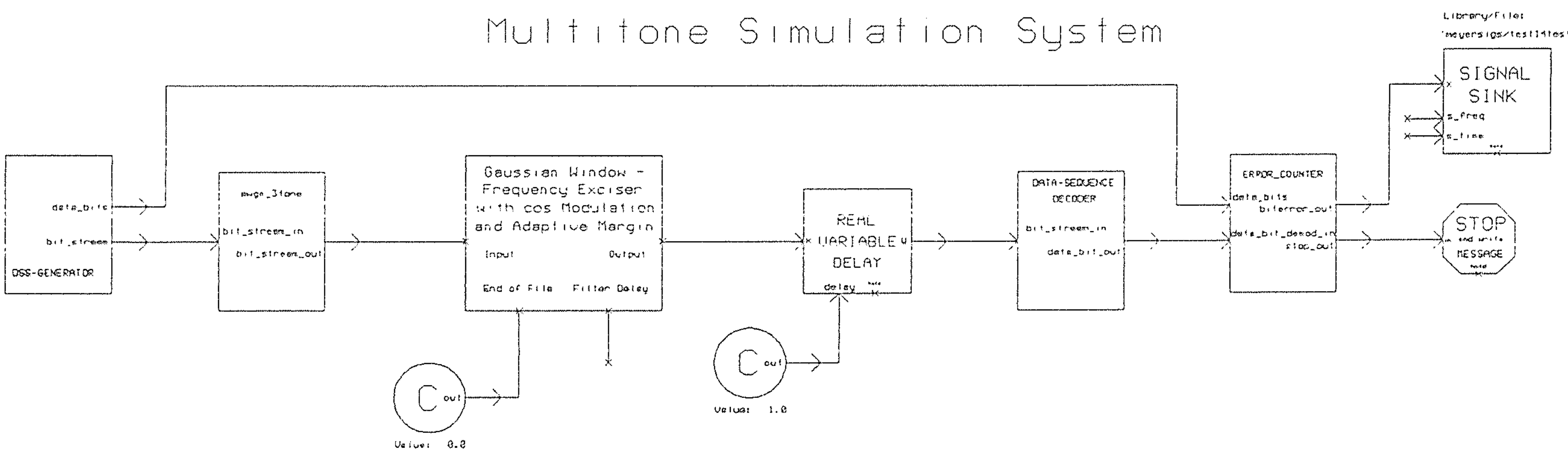

Figure A.4 The Simulation System for Multitone Interference Cancellation

Parameter	Value
Signal Source	
Data Bitrate	1 Bits/sec
Data Sampling Rate	63 Hz
PN-Sequence Bitrate	1 Bits/sec
PN-Sequence Sampling Rate	1 Hz
Channel	
FM-Carrier Frequency	0 Hz
FM-Frequency Deviation	20 Hz/Volt
FM-Amplitude	14.14 Volt
Message Frequency	2 Hz
Message Amplitude	1 Volt
Sampling Frequency	63 Hz

Table A.2 The Simulation System Parameters for Direct Sequence Spread Spectrum Digital Audio Broadcasting

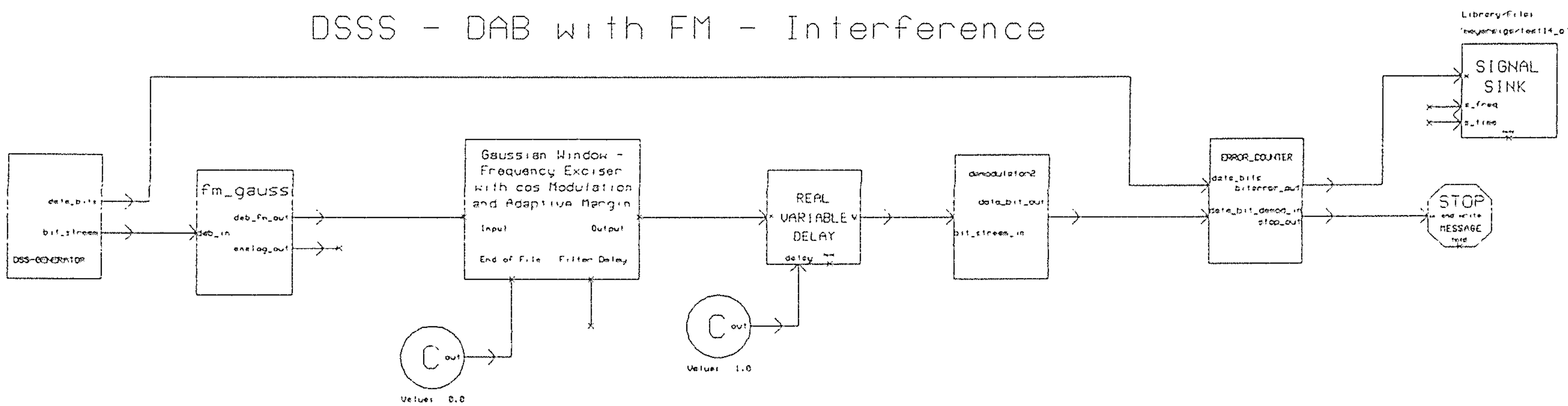

Figure A.5 The Simulation System for Direct Sequence Spread Spectrum Digital Audio Broadcasting

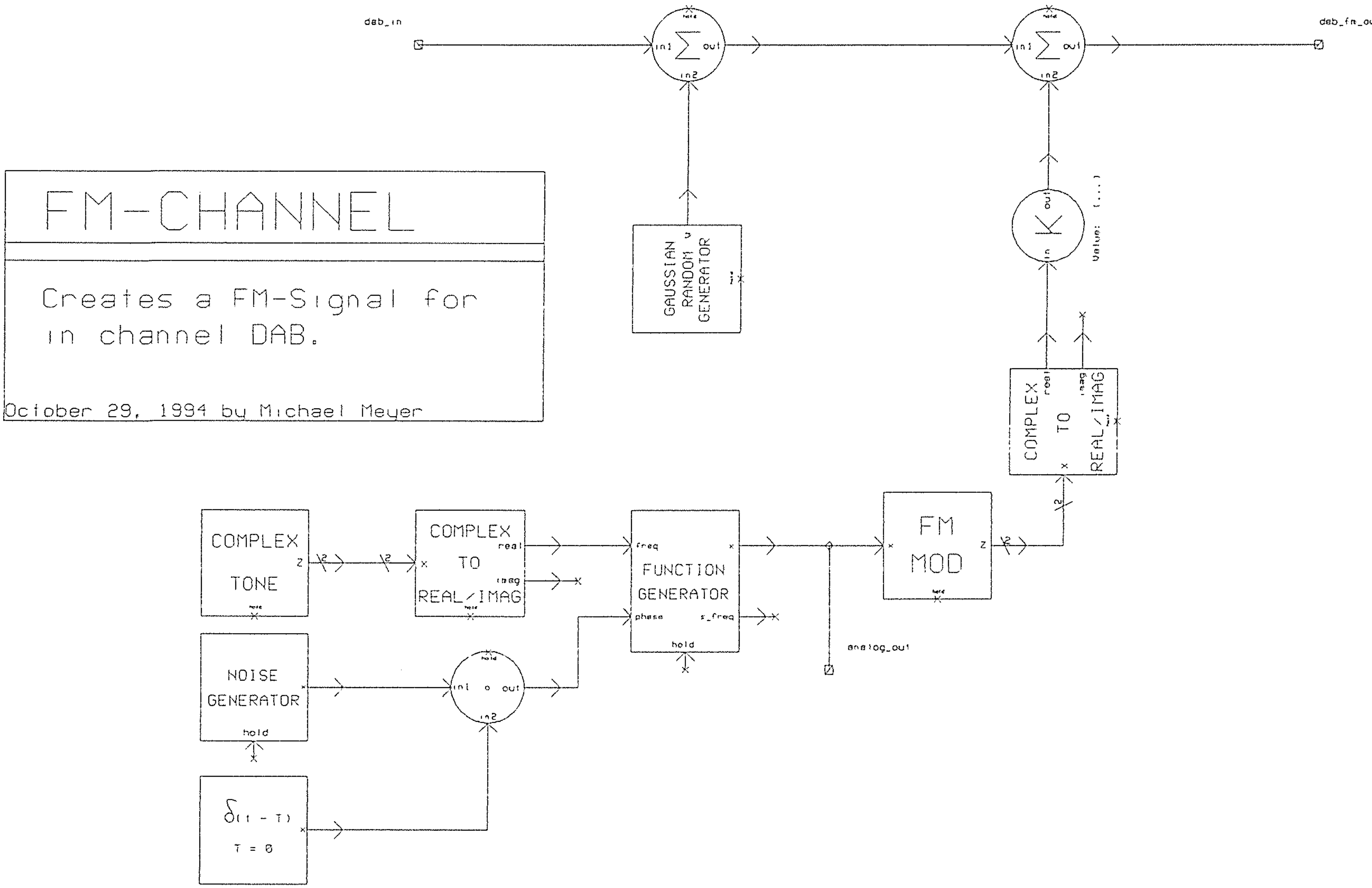

Figure A.6 The FM Channel for the DSSS DAB System

Parameter	**Value**
Signal Source	
Data Bitrate	1 Bits/sec
Data Sampling Rate	63 Hz
PN-Sequence Bitrate	1 Bits/sec
PN-Sequence Sampling Rate	1 Hz
Channel	
FM-Carrier Frequency	0 Hz
FM-Frequency Deviation	20 Hz/Volt
FM-Amplitude	14.14 Volt
Message Frequency	2 Hz
Message Amplitude	1 Volt
Sampling Frequency	63 Hz

Table A.3 The Signal to Noise and Interference Ratio Simulation Parameters

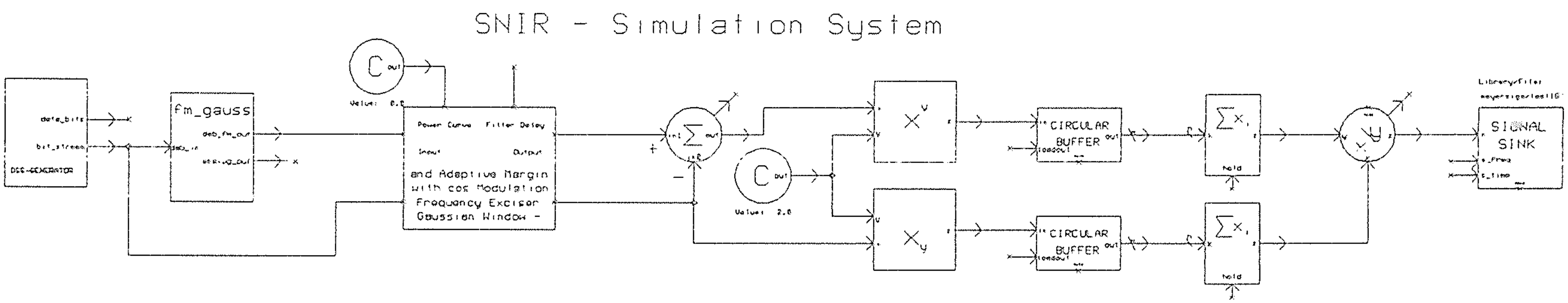

Figure A.7 The Signal to Noise and Interference Ratio Simulation System

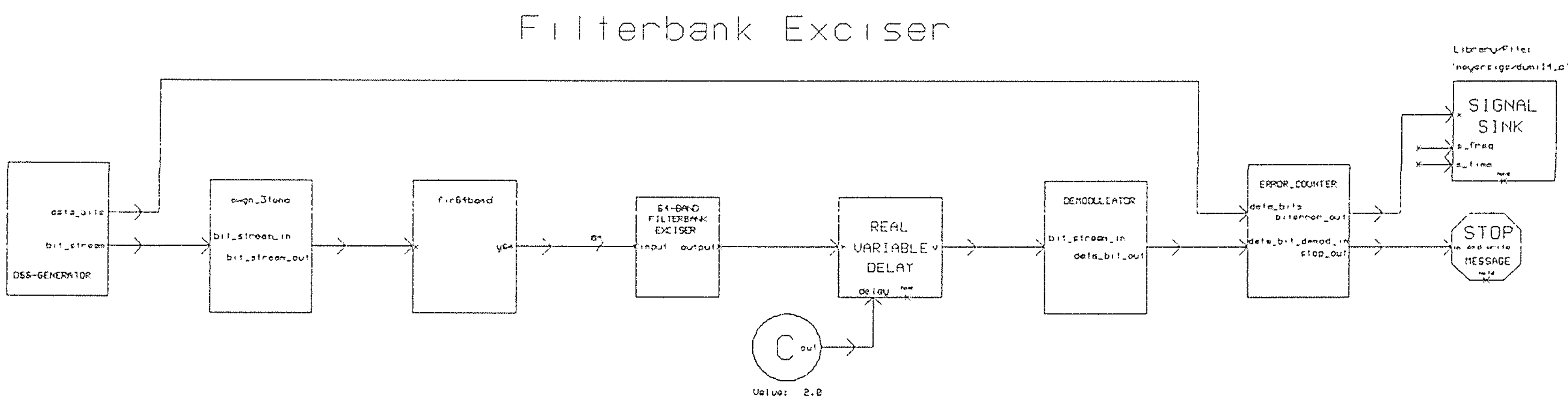

Figure A.8 64-Band Subband Exciser System

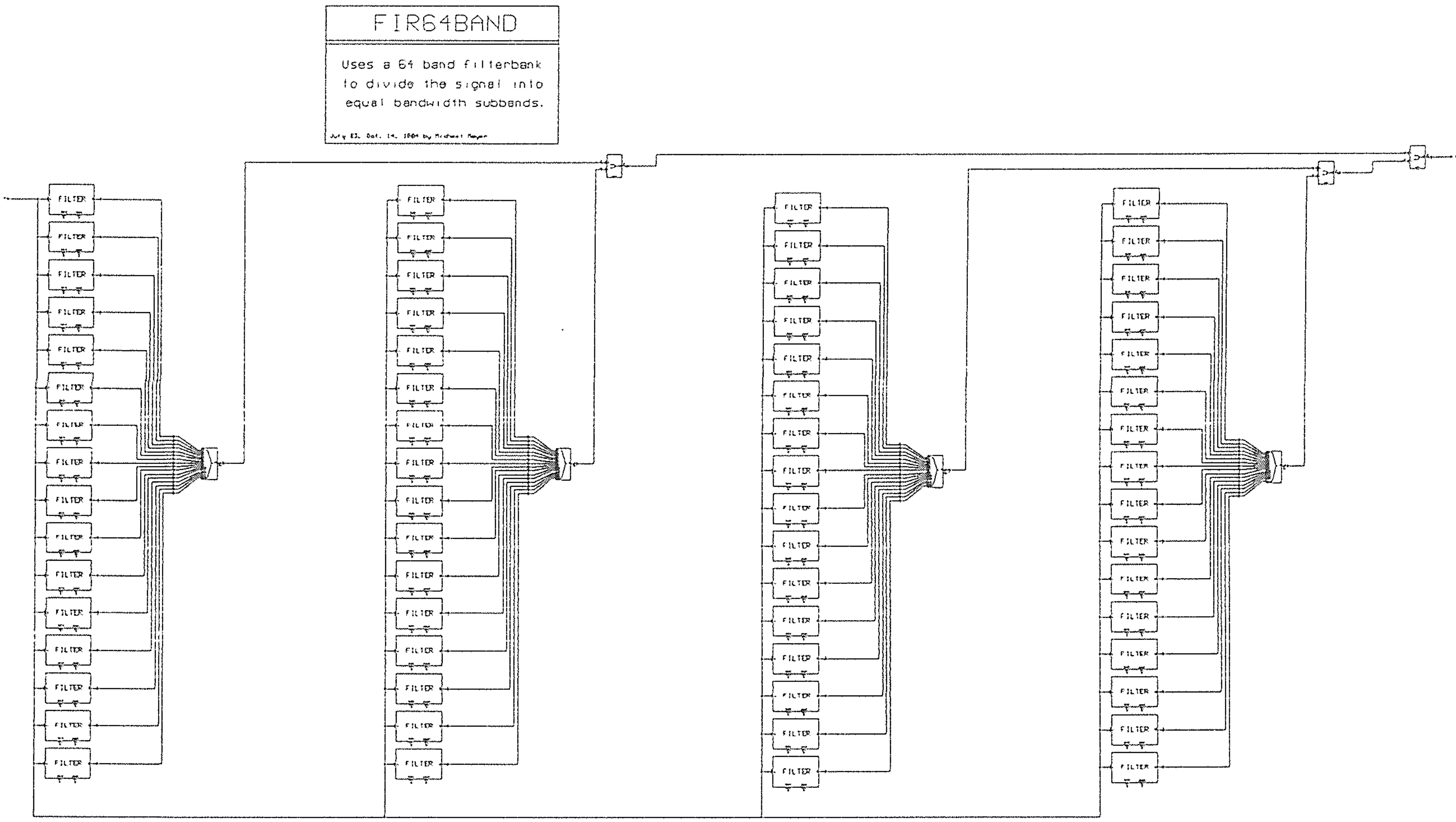

Figure A.9 64 Band Filterbank

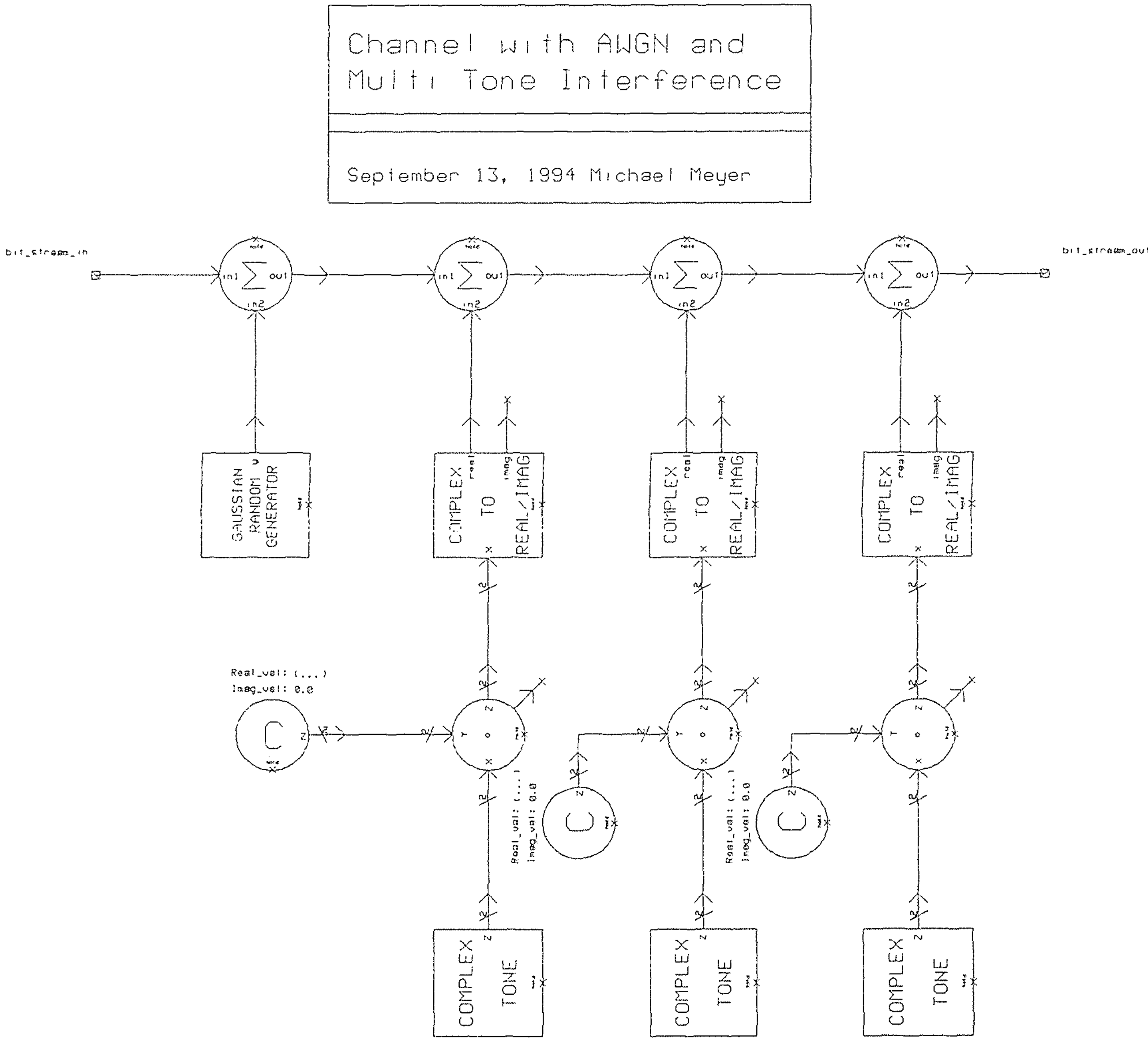

Figure A.10 Channel with Multitone Interference and AWGN

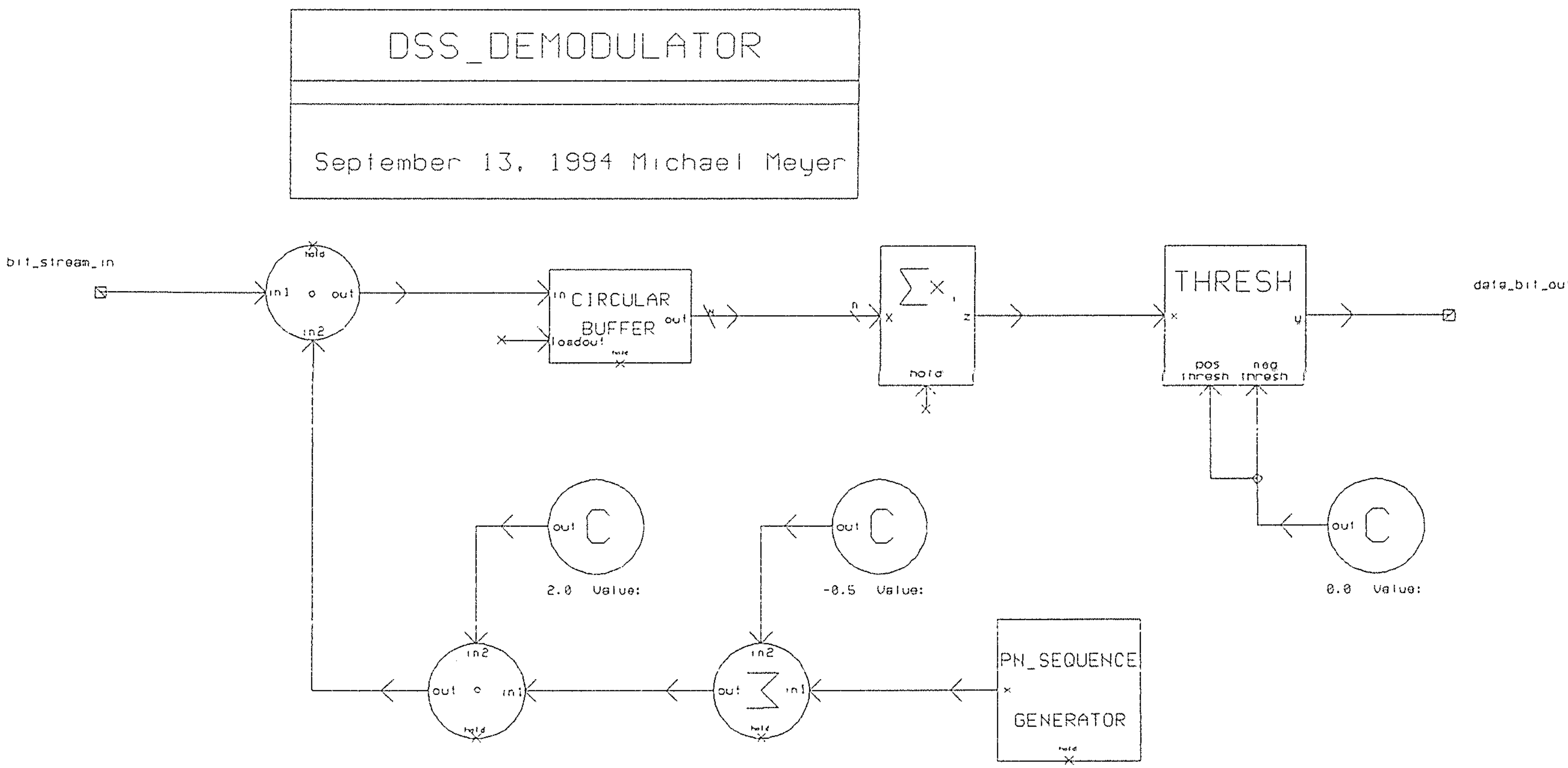

Figure A.11 DSS Demodulator

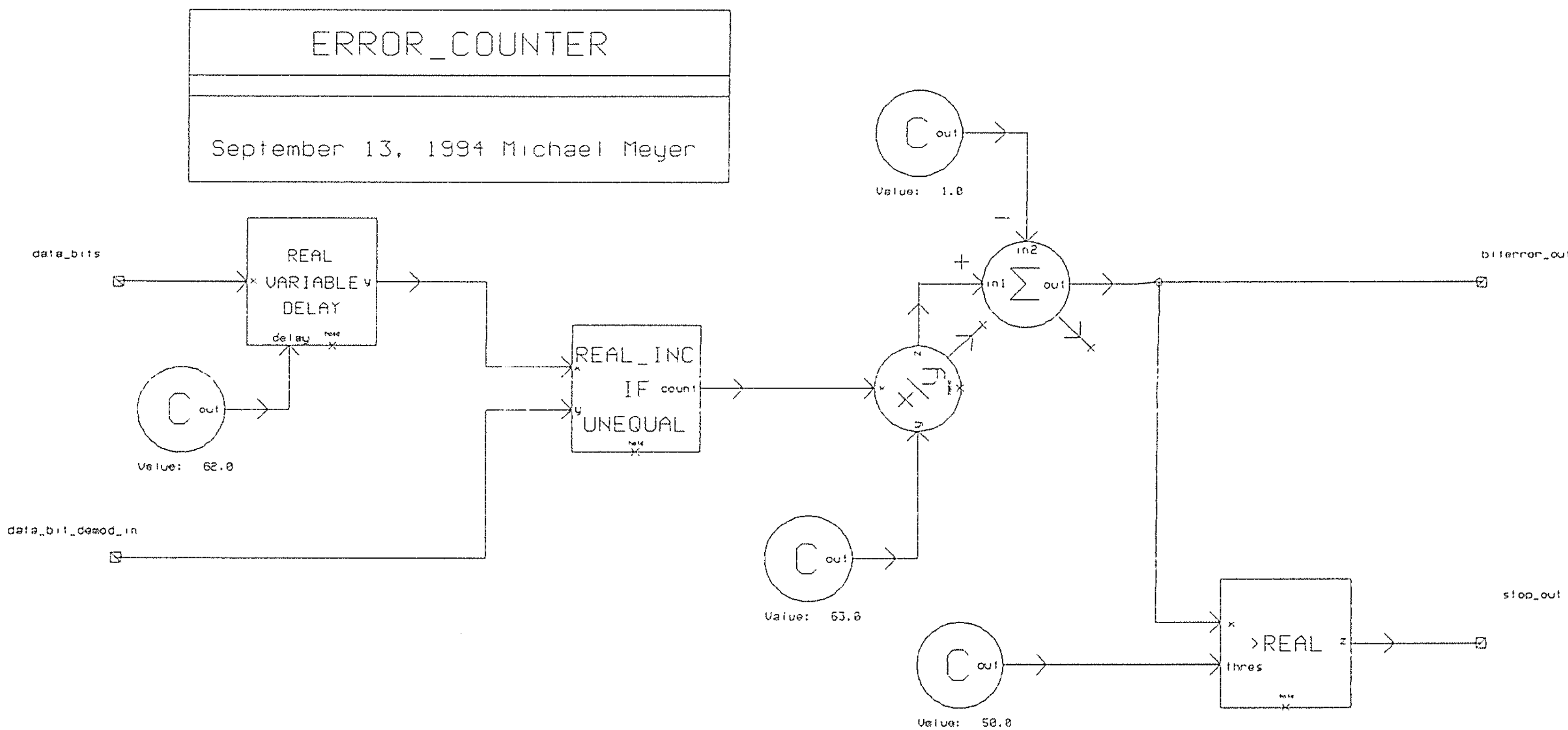

Figure A.12 Error Counter

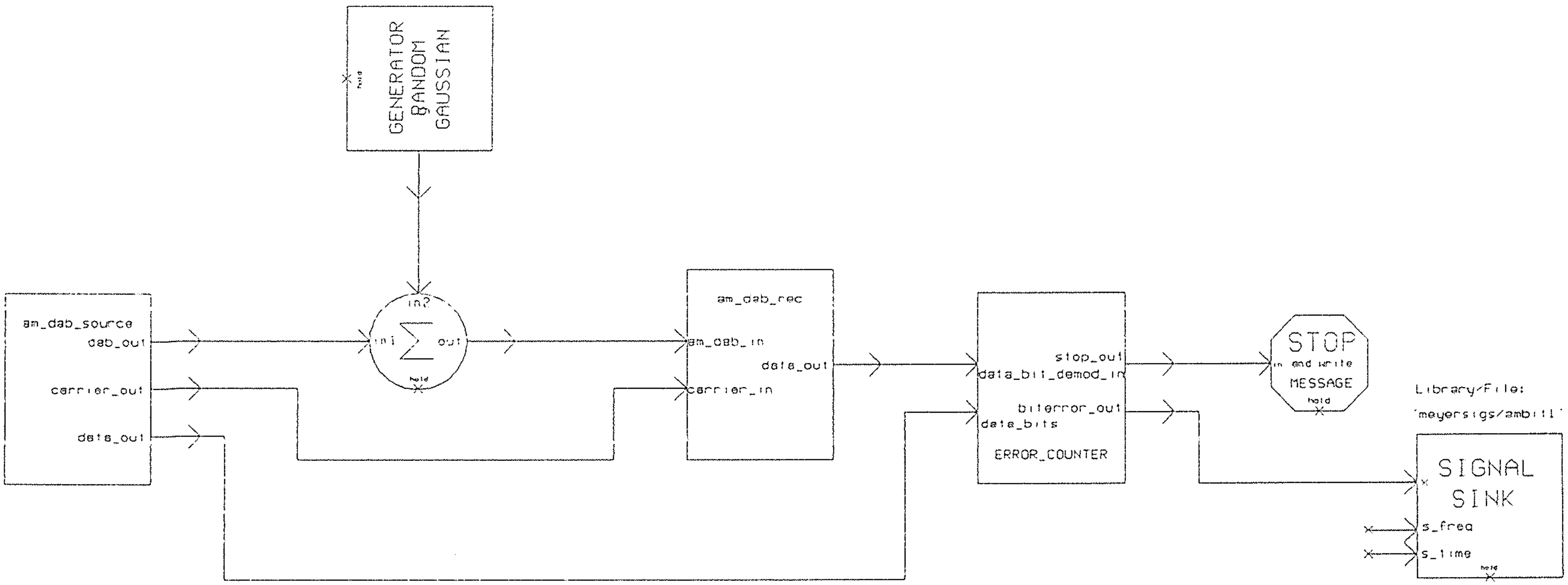

Figure A.13 DAB on AM Simulation System

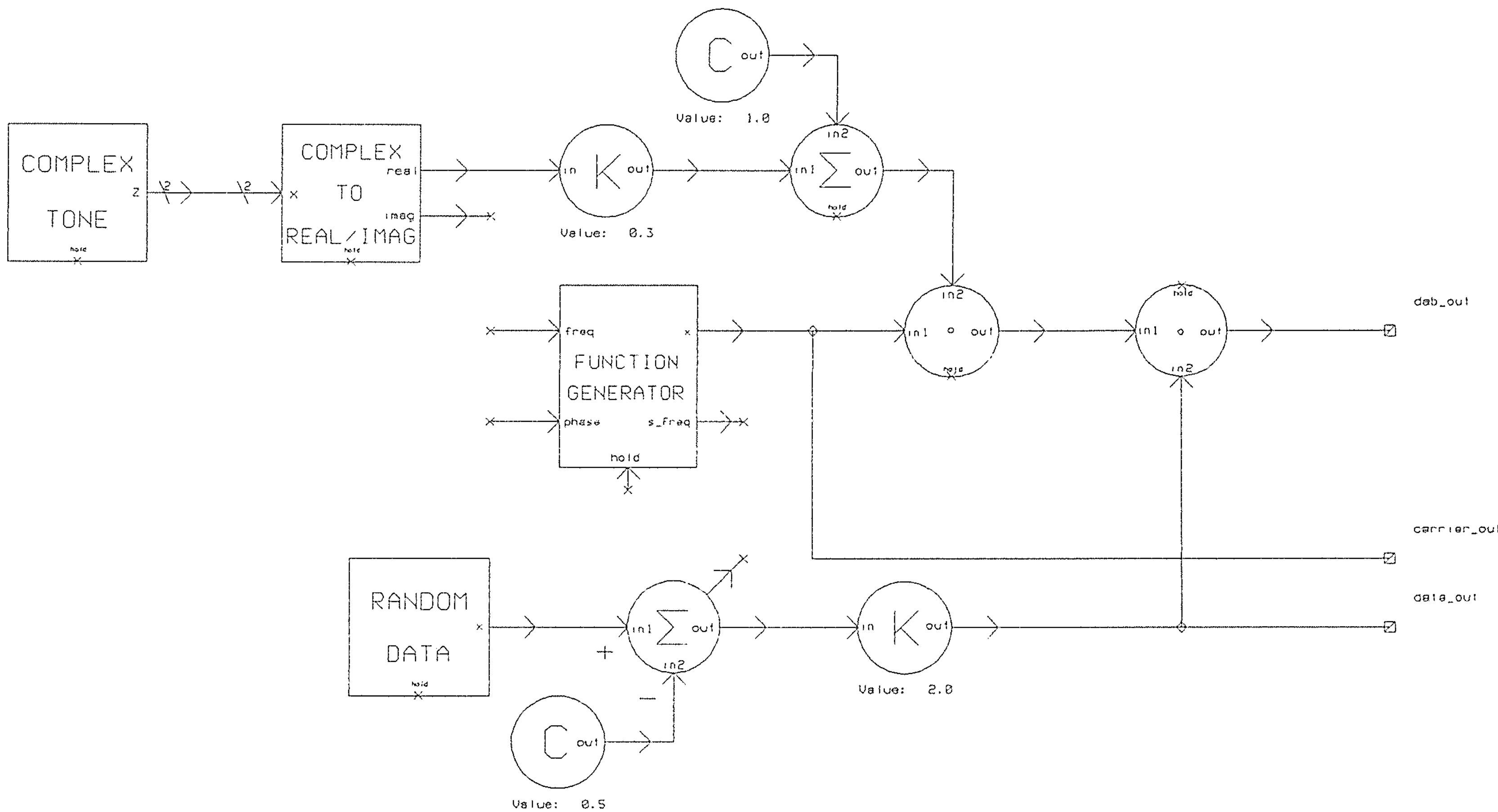

Figure A.14 AM DAB Transmitter

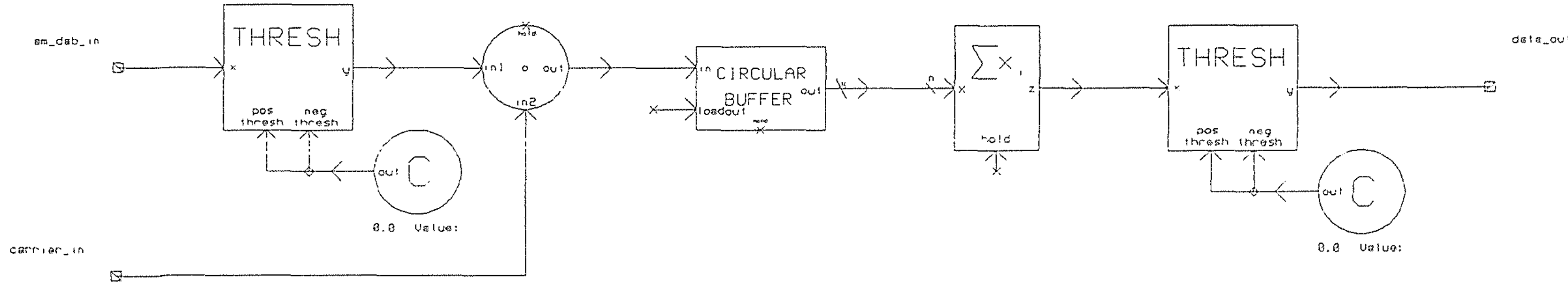

Figure A.15 AM DAB Receiver for the DAB Signal

REFERENCES

1. A. N. Akansu and Y. Liu, "On signal decomposition techniques," *Optical Engineering*, pp. 912–920, July 1991.

2. A. N. Akansu and R. A. Haddad, *Multiresolution Signal Decomposition, Transforms, Subbands, Wavelets*, Academic Press, INC., San Diego, California, 1992.

3. R. C. Dixon, *Spread Spectrum Systems*, John Wiley & Sons, New York, second ed., 1984.

4. R. Gold, "Maximal recursive sequences with 3-valued recursive cross-correlation functions," *IEEE Transactions on Information*, January 1968.

5. S. W. Golomb *et al.*, *Shift Register Sequences*, Aegean Parc Press, Laguna Hills, California, revised ed., 1982.

6. R. A. Haddad, "A class of orthogonal nonrecursive binomial filters," *IEEE Transactions on Audio and Electroacoustics*, pp. 296–304, December 1971.

7. R. A. Haddad, A. N. Akansu, and A. Benyassine, "Time-frequency localization in transforms, subbands, and wavelets: a critical review," *Optical Engineering*, pp. 1411–1428, July 1993.

8. S. Haykin, *Communication Systems*, John Wiley & Sons, New York, New York, second ed., 1983.

9. D. L. W. Hinderks, "Digital audio broadcasting - current and future directions," in *Applications of Subbands and Wavelets*, NJIT, Department of Electrical and Computer Engineering, Center for Communications and Signal Processing Research, March 1994.

10. B. P. Lathi, *Modern Digital and Analog Communication Systems*, CBS College Publishing, New York, NJ, 1983.

11. E. A. Lee and D. G. Messerschmitt, *Digital Communications*, Kluwer Academic Publisher, Boston, second ed., 1994.

12. M. Medley, G. J. Saulnier, and P. Das, "Applications of the wavelet transform in spread spectrum communications systems," in *Applications of Subbands and Wavelets*, NJIT, Department of Electrical and Computer Engineering, Center for Communications and Signal Processing Research, March 1994.

13. M. Meyer, M. V. Tazebay, and A. N. Akansu, "A sliding and variable window based multitone excision for digital audio broadcast," *submitted to IEEE International Symposium on Circuits and Systems*, April 1995.

14. A. Polydoros, "In-band on-channel digital audio broadcast: Review of existing proposals and further suggestions," *Report No: S0492-1*, April 1992.

15. D. V. Sarwate and M. B. Pursley, "Crosscorrelation properties of pseudorandom and related sequences," *Proceedings of the IEEE*, May 1980.

16. H. Taub and D. L. Schilling, *Principles of Communication Systems*, Mc Graw-Hill Publishing Company, New York, New York, second ed., 1986.

17. M. V. Tazebay and A. N. Akansu, "Adaptive subband transforms in time-frequency excisers for dsss communications systems," *submitted to IEEE Transactions on Signal Processing*, July 1994.

18. M. V. Tazebay and A. N. Akansu, "Progressive optimization of time-frequency localization in subband trees," in *IEEE International Symposium on Time-Frequency and Time-Scale Analysis*, pp. 128–131, The IEEE Signal Processing Society and The IEEE Philadelphia Section, October 1994.

19. M. V. Tazebay, A. N. Akansu, and M. J. Sherman, "A novel adaptive time-frequency excision technique for direct sequence spread spectrum communications," in *IEEE International Symposium on Time-Frequency and Time-Scale Analysis*, pp. 492–495, The IEEE Signal Processing Society and The IEEE Philadelphia Section, October 1994.

20. M. V. Tazebay, A. Benyassine, and A. N. Akansu, "Time-frequency localization in subband trees and progressive optimality," *submitted to IEEE Transactions on Signal Processing*, January 1994.

21. K. Thompson and D. Whipple, "Concepts of CDMA," in *Wireless Communications Symposium*, pp. 13–24, Hewlett-Packard Company, 1994.

22. P. P. Vaidyanathan, *Multirate Systems and Filter Banks*, Prentice-Hall, Inc., Englewood Cliffs, New Jersey, 1993.

23. D. P. Whipple, "The CDMA standard," *Applied Microwave & Wireless*, 1994.

24. R. E. Ziemer and R. L. Peterson, *Digital Communications and Spread Spectrum Systems*, Macmillan Publishing Company, New York, New York, 1985.

25. R. E. Ziemer and R. L. Peterson, *Introduction to Digital Communication*, Macmillan Publishing Company, New York, New York, 1992.